CoCoNuTs: A diverse subclass of Type IV restriction systems predicted to target RNA

Ryan T. Bell[1,*], Harutyun Sahakyan[1], Kira S. Makarova[1], Yuri I. Wolf[1], Eugene V. Koonin[1,*]

[1]National Center for Biotechnology Information, National Library of Medicine, National Institutes of Health, Bethesda, MD 20894, USA

*Correspondence to: Ryan T. Bell (ryan.bell@nih.gov) or Eugene V. Koonin (koonin@ncbi.nlm.nih.gov)

Abstract

A comprehensive census of McrBC systems, among the most common forms of prokaryotic Type IV restriction systems, followed by phylogenetic analysis, reveals their enormous abundance in diverse prokaryotes and a plethora of genomic associations. We focus on a previously uncharacterized branch, which we denote CoCoNuTs (coiled-coil nuclease tandems) for their salient features: the presence of extensive coiled-coil structures and tandem nucleases. The CoCoNuTs alone show extraordinary variety, with 3 distinct types and multiple subtypes. All CoCoNuTs contain domains predicted to interact with translation system components, such as OB-folds resembling the SmpB protein that binds bacterial tmRNA, YTH-like domains that might recognize methylated tmRNA, tRNA, or rRNA, and RNA-binding Hsp70 chaperone homologs, along with RNases, such as HEPN domains, all suggesting that the CoCoNuTs target RNA. Many CoCoNuTs might additionally target DNA, via McrC nuclease homologs. Additional restriction systems, such as Type I RM, BREX, and Druantia Type III, are frequently encoded in the same predicted superoperons. In many of these superoperons, CoCoNuTs are likely regulated by cyclic nucleotides, possibly, RNA fragments with cyclic termini, that bind associated CARF (CRISPR-Associated Rossmann Fold) domains. The CoCoNuTs, together with the ancillary restriction factors, might employ an echeloned defense strategy analogous to that of Type III CRISPR-Cas systems, in which an immune response eliminating virus DNA and/or RNA is launched first, but then, if it fails, an abortive infection response leading to PCD/dormancy via host RNA cleavage takes over.

Introduction

All organisms are subject to an incessant barrage of genetic parasites, such as viruses and transposons. Over billions of years, the continuous arms race between hosts and parasites drove the evolution of immense, intricately interconnected networks of diverse defense systems and pathways (Burroughs et al., 2015, Gao et al., 2020, Goldfarb et al., 2015, Bell et al., 2020, Koonin and Aravind, 2002, Swarts et al., 2014). In particular, in the last few years, targeted searches for defense systems in prokaryotes, typically capitalizing on the presence of variable genomic defense islands, have dramatically expanded their known diversity and led to the discovery of a plethora of biological conflict strategies and mechanisms (Gao et al., 2020, Bell et al., 2020, Anantharaman et al., 2012, Kaur et al., 2020).

One of the most ancient and common forms of defense against mobile genetic elements (MGE) is the targeted restriction of nucleic acids. Since the initial discovery of this activity among strains of bacteria resistant to certain viruses, myriad forms of recognition and degradation of nucleic acids have been described, in virtually all life forms. Characterization of the most prominent of these systems, such as restriction-modification (RM), RNA interference (RNAi), and CRISPR-Cas (clustered regularly interspaced short palindromic repeats-CRISPR associated genes), has led to the development of a profusion of highly effective experimental and therapeutic techniques, in particular, genome editing and engineering (Loenen et al., 2014, Fire et al., 1998, Agrawal et al., 2003, Makarova et al., 2006, Makarova et al., 2020b, Gasiunas et al., 2012, Jinek et al., 2012).

Historically, the two-component McrBC (modified cytosine restriction) system was the first form of restriction to be described, although the mechanism remained obscure for decades, and for a time, this system was referred to as RglB (restriction of glucoseless phages) due to its ability to restrict T-even phage DNA which contained hydroxymethylcytosine, but not glucosylated bases (Raleigh et al., 1989, Luria and Human, 1952, Fleischman et al., 1976, Dila et al., 1990). Today, the prototypical McrBC system, native to *E. coil* K-12, is considered a Type IV (modification-dependent) restriction system that degrades DNA containing methylcytosine (5mC) or hydroxymethylcytosine (5hmC), with a degree of sequence context specificity (Sutherland et al., 1992, Sukackaite et al., 2012).

Type IV restriction enzymes contain at least two components: 1) a dedicated specificity domain that recognizes modified DNA, and 2) an endonuclease domain that cleaves the target (Weigele and Raleigh, 2016, Loenen et al., 2014). In the well-characterized example from *E. coli* K-12, McrB harbors an N-terminal DUF(domain of unknown function)3578 that recognizes methylcytosine. We denote this domain, as its function is not unknown, as ADAM (a domain with an affinity for methylcytosine). The ADAM domain is fused to a GTPase domain of the AAA+ ATPase superfamily, the only known GTPase in this clade, which is believed to translocate DNA (Figure 1 A, B, C) (Sutherland et al., 1992, Iyer et al., 2004, Nirwan et al., 2019, Panne et al., 1999). McrC, encoded by a separate gene in the same operon, contains an N-terminal DUF2357 domain, which interacts with the GTPase domain in McrB and stimulates its activity, and is

71 fused to a PD-(D/E)xK superfamily endonuclease (Figure 1 A, B, D) (Niu et al., 2020, Sutherland
72 et al., 1992).

73 Our recent analysis of the modified base-binding EVE (named for Protein Data Bank
74 (PDB) structural identifier 2eve) domain superfamily demonstrated how the distribution of the
75 EVE-like domains connects the elaborate eukaryotic RNA regulation and RNA interference-
76 related epigenetic silencing pathways to largely uncharacterized prokaryotic antiphage
77 restriction systems (Bell et al., 2020). EVE superfamily domains, which in eukaryotes recognize
78 modified DNA or RNA as part of mRNA maturation or epigenetic silencing functions, are often
79 fused to McrB-like GTPases in prokaryotes, and indeed, these are the most frequently occurring
80 EVE-containing fusion proteins (Bell et al., 2020). These observations motivated us to conduct a
81 comprehensive computational search for McrBC systems, followed by a census of all associated
82 domains, to chart the vast and diverse population of antiviral specificity modules, vital for
83 prokaryotic defense, that also provided important source material during the evolution of
84 central signature features of eukaryotic cells. Here we present the results of this census and
85 describe an extraordinary, not previously appreciated variety of domain architectures of the
86 McrBC family of Type IV restriction systems. In particular, we focus on a major McrBC branch
87 that we denote coiled-coil nuclease tandem (CoCoNuT) systems, which we explore in detail.

88

89 Results and Discussion

90 *Comprehensive census of McrBC systems*

91 The search for McrBC systems included PSI-BLAST runs against the non-redundant
92 protein sequence database at the NCBI, followed by several filtering strategies (see Methods)
93 to obtain a clean set of nearly 34,000, distributed broadly among prokaryotes (Figure 1 E).

-

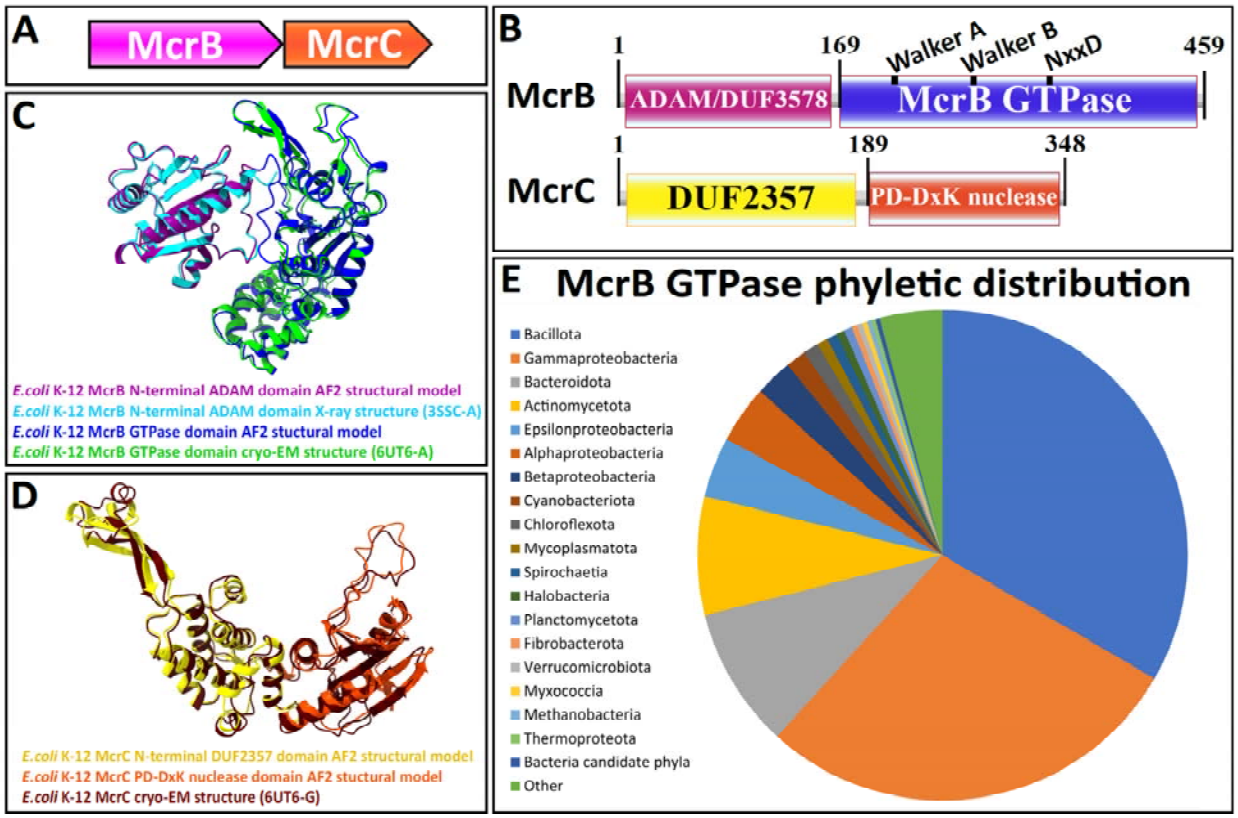

Figure 1: Genetic organization, signature sequence motifs, structural models, and phyletic distribution of McrB GTPases detected in this work

A) McrBC is a two-component restriction system with each component typically (except for extremely rare gene fusions) encoded by a separate gene expressed as a single operon, depicted here and in subsequent figures as arrows pointing in the direction of transcription. In most cases, McrB is the upstream gene in the operon. B) In the prototypical *E.coli* K-12 McrBC system, McrB contains an N-terminal methylcytosine-binding domain, ADAM/DUF3578, fused to a GTPase of the AAA+ ATPase clade (Sukackaite et al., 2012). This GTPase contains the Walker A and Walker B motifs that are conserved in P-loop NTPases as well as a signature NxxD motif, all of which are required for GTP hydrolysis (Nirwan et al., 2019, Niu et al., 2020, Pieper et al., 1999). McrC consists of a PD-DxK nuclease and an N-terminal DUF2357 domain, which comprises a helical bundle with a stalk-like extension that interacts with and activates individual McrB GTPases while they are assembled into hexamers (Niu et al., 2020, Nirwan et al., 2019). C) AlphaFold2 structural model of *E. coli* K-12 ADAM-McrB GTPase fusion protein monomer and separate X-ray diffraction and cryo-EM structures of the ADAM and GTPase domains (Niu et al., 2020, Sukackaite et al., 2012). D) AlphaFold2 structural model and cryo-EM structure of *E. coli* K-12 McrC monomer with DUF2357-PD-D/ExK architecture (Niu et al., 2020). The structures were visualized with ChimeraX (Pettersen et al., 2021). E) Phyletic distribution of McrB GTPase homologs detected in this work, each found in a genomic island with distinct domain composition, clustered to a similarity threshold of 0.9, then assigned a weight inversely proportional to the cluster size (see Methods).

In the subsequent phase of analysis, GTPase domain sequences were extracted from the McrB homolog pool, and DUF2357 and PD-D/ExK nuclease domain sequences were extracted

from the McrC homolog pool, leaving as a remainder the fused specificity domains that we intended to classify (although the McrC homologs are not the primary bearers of specificity modules in McrBC systems, they can be fused to various additional domains, including those of the EVE superfamily) (Figure 2, Supplementary Figure S1). Unexpectedly, we found that both the GTPase domains and DUF2357 domains frequently contained insertions into their coding sequences, likely encoding specificity domains and coiled-coils, respectively.

Removing variable inserts from the conserved McrBC domains allowed accurate, comprehensive phylogenetic analysis of the McrB GTPase (Figure 2) and McrC DUF2357 (Supplementary Figure S1) families. These two trees were generally topologically concordant and revealed several distinct branches not previously recognized. The branch containing the prototypical McrBC system from *E. coil* K-12 (blue in Figure 2) is characterized by frequent genomic association with Type I RM systems, usually with unidirectional gene orientations and the potential of forming a single operon (Raleigh, 1992). This branch and others, which exhibit two particularly prevalent associations, with a DISARM-like antiphage system (green in Figure 2) (Ofir et al., 2018), and, surprisingly for a Type IV restriction system, with predicted DNA methyltransferases (red in Figure 2), will be the subject of a separate, forthcoming publication.

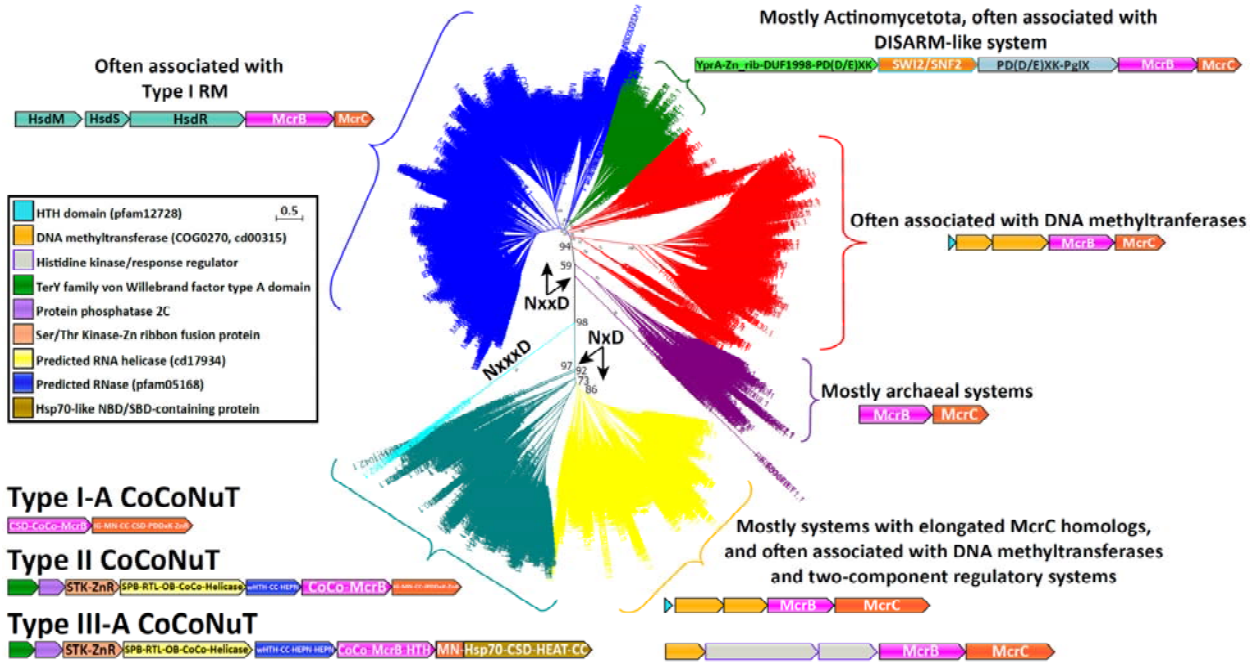

Figure 2: Phylogenetic tree of the McrB GTPases

The major clades in the phylogenetic tree of the McrB GTPases are distinguished by the distinct versions of the Nx(xx)D signature motif. The teal and yellow groups, with bootstrap support of 97%, have an NxD motif, whereas the blue, green, red, and purple groups, with variable bootstrap support, have an NxxD motif, indicated by the arrows; the sequences in the smaller, cyan clade, with 98% bootstrap support, have an NxxxD motif. Each of the differently colored groups is characterized by distinct conserved genomic associations that are abundant within

141 but not completely confined to the respective groups. This tree was built from the representatives of 90% identity
142 clusters of all validated homologs. Abbreviations of domains: McrB – McrB GTPase domain; CoCo/CC – coiled-coil;
143 MN – McrC N-terminal domain (DUF2357); CSD – cold shock domain; IG – Immunoglobulin (IG)-like beta-sandwich
144 domain; ZnR – zinc ribbon domain; SPB – SmpB-like domain; RTL – RNase toxin-like domain; HEPN – HEPN family
145 nuclease domain; OB – OB-fold domain; iPD-D/ExK – inactivated PD-D/ExK fold; Hsp70-like ATPase – Hsp70-like
146 NBD/SBD; HEAT – HEAT-like helical repeats; YprA – YprA-like helicase domain; DUF1998 - DUF1998 is often found
147 in or associated with helicases and contains four conserved, putatively metal ion-binding cysteine residues;
148 SWI2/SNF2 – SWI2/SNF2-family ATPase; PglX – PglX-like DNA methyltransferase; HsdR/M/S – Type I RM system
149 restriction, methylation, and specificity factors.

150

151 *A variant of the McrB GTPase signature motif distinguishes a large group of unusual*
152 *McrBC systems*

153 A major branch (teal and yellow in Figure 2) of the McrBC family is characterized by a
154 conserved deletion within the NxxD GTPase signature motif (where x is any amino acid), found
155 in all McrB-like GTPases, reducing it to NxD (Figure 1 B, Figure 2) (Neuwald et al., 1999, Iyer et
156 al., 2004, Erzberger and Berger, 2006, Niu et al., 2020). No NxD motif McrB GTPase has been
157 characterized, but the extensive study of the NxxD motif offers clues to the potential impact of
158 the motif shortening. The asparagine (N) residue is strictly required for GTP binding and
159 hydrolysis (Pieper et al., 1999). As this residue is analogous to sensor-1 in ATP-hydrolyzing
160 members of the AAA+ family, it can be predicted to position a catalytic water molecule for
161 nucleophilic attack on the γ-phosphate of an NTP (Erzberger and Berger, 2006, Colicelli, 2004,
162 Bourne et al., 1991, Niu et al., 2020, Pieper et al., 1999). A recent structural analysis has shown
163 that the aspartate (D) interacts with a conserved arginine/lysine residue in McrC which, via a
164 hydrogen-bonding network, resituates the NxxD motif in relation to its interface with the
165 Walker B motif such that, together, they optimally position a catalytic water to stimulate
166 hydrolysis (Niu et al., 2020). Accordingly, the truncation of this motif might be expected to
167 modulate the rate of hydrolysis, and potentially compel functional association with only a
168 subset of McrC homologs containing compensatory mutations. The NxD branch is characterized
169 by many McrC homologs with unusual features, such as predicted RNA-binding domains, that
170 might not be compatible with conventional McrB GTPases from the NxxD clade, which often
171 occur in the same genomes (see below).

172 Many of these NxD GTPases are contextually associated with DNA methyltransferases,
173 like the NxxD GTPases, but are distinguished by additional complexity in the domains fused to
174 the McrC homologs and the frequent presence of two-component regulatory system genes in
175 the same operon (yellow in Figure 2). We also detected a small number of GTPases with an
176 insertion in the signature motif (cyan in Figure 2), expanding it to NxxxD, which are
177 methyltransferase-associated as well. This association is likely to be ancestral, as it is found in
178 all 3 branches of the McrB GTPase tree with different signature motif variations.

179 The most notable feature of the NxD branch of GTPases is a large clade characterized by
180 fusion to long coiled-coil domains (teal in Figure 2, Supplementary Table S1), a derived and

181 distinctly different architecture from the small, modular DNA-binding specificity domains
182 typically found in canonical McrB homologs. The McrC homologs associated with these coiled-
183 coil McrB GTPase fusions also often lack the PD-D/ExK endonuclease entirely or contain an
184 AlphaFold2 (AF2)-predicted endonuclease fold with inactivating replacements of catalytic
185 residues (Supplementary Table S1). However, in the cases where the McrC nuclease is missing
186 or likely inactive, these systems are always encoded in close association, often with overlapping
187 reading frames, with HEPN (higher eukaryotes and prokaryotes nucleotide-binding)
188 ribonuclease domains, or other predicted nucleases (Figure 3, Supplementary Figure S2) (Pillon
189 et al., 2021). Based on these features of domain architecture and genomic context, we denote
190 these uncharacterized McrBC-containing operons coiled-coil nuclease tandem (CoCoNuT)
191 systems.

192 The deepest branching group of the NxD GTPase systems is typified by a fusion of an
193 Hsp70-like ATPase nucleotide-binding domain and substrate-binding domain (NBD/SBD) to the
194 McrB GTPase domain (purple in Figure 3, Supplementary Figure S2, Supplementary Table S1).
195 Hsp70 is an ATP-dependent protein chaperone that binds exposed hydrophobic peptides and
196 facilitates protein folding (Mayer, 2021). It also associates with AU-rich mRNA, and in some
197 cases, such as the bacterial homolog DnaK, C-rich RNA, an interaction involving both the NBD
198 and SBD (Kishor et al., 2017, Zimmer et al., 2001, Kishor et al., 2013). These systems might be
199 functionally related to the CoCoNuTs, given that an analogous unit is encoded by a type of
200 CoCoNuT system where similar domains are fused to the McrC homolog rather than to the
201 McrB GTPase homolog (see below). In another large clade of CoCoNuT-like systems, the GTPase
202 is fused to a domain homologous to FtsB, an essential bacterial cell division protein containing
203 transmembrane and coiled-coil helices (Supplementary Figure S2, Supplementary Table S1)
204 (Khadria and Senes, 2013). They are associated with signal peptidase family proteins likely to
205 function as pilus assembly factors (Supplementary Table S1) [47] and usually contain coiled-coil
206 domains fused to both the McrB and McrC homologs. Therefore, we denote them coiled-coil
207 and pilus assembly linked to McrBC (CoCoPALM) systems (Supplementary Figure S2).

208 Here, we focus on the CoCoNuTs, whereas the CoCoPALMs and the rest of the NxD
209 GTPase methyltransferase-associated homologs will be explored in a separate, forthcoming
210 publication.

211

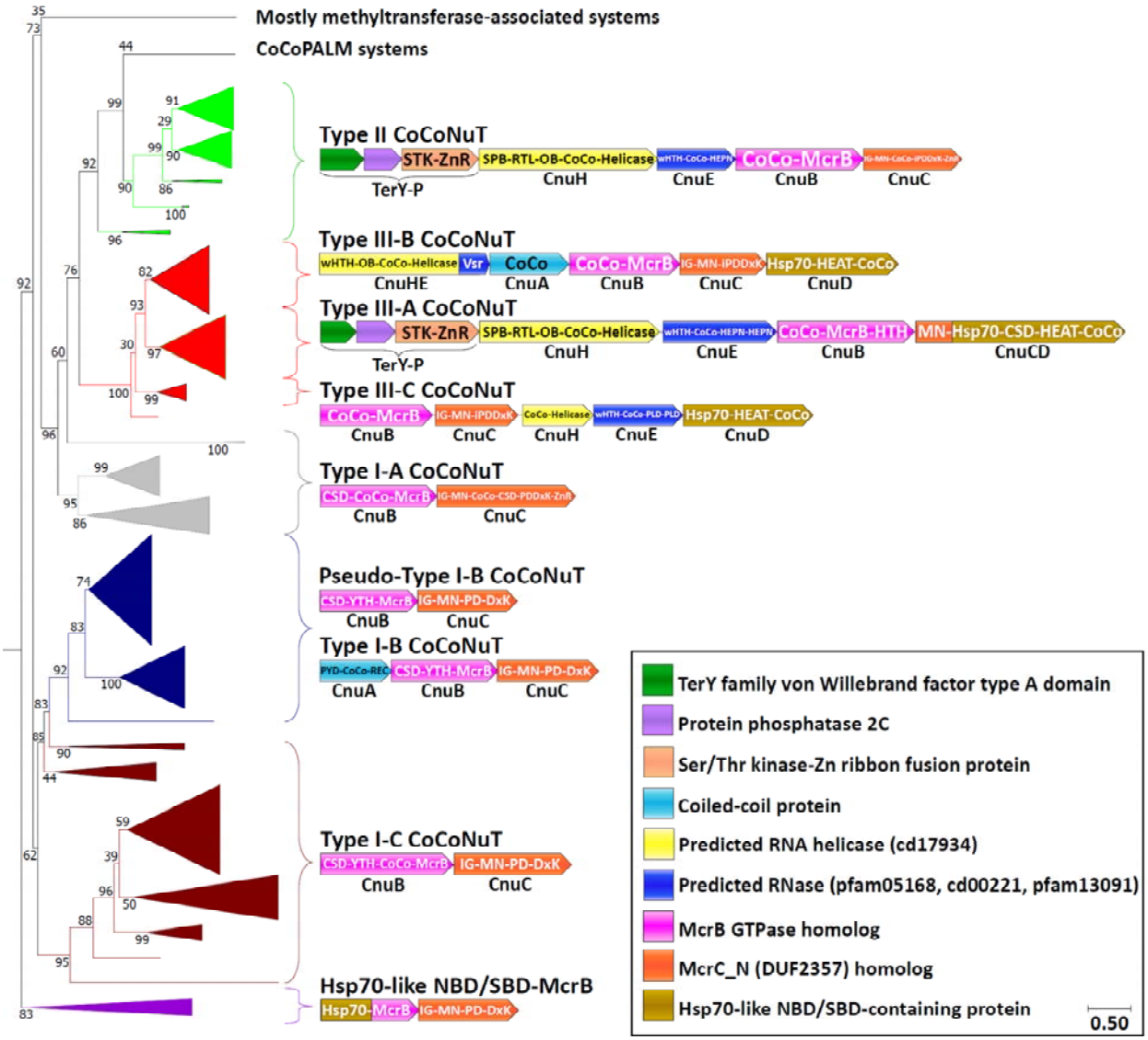

Figure 3: CoCoNuT system phylogeny and classification

The figure shows the detailed phylogeny of McrB GTPases from CoCoNuT systems and their close relatives. All these GTPases possess an NxD GTPase motif rather than NxxD. This tree was built from the representatives of 90% clustering of all validated homologs. Abbreviations of domains: McrB – McrB GTPase domain; CoCo – coiled-coil; MN – McrC N-terminal domain (DUF2357); CSD – cold shock domain; YTH – YTH-like domain; IG – Immunoglobulin (IG)-like beta-sandwich domain; Hsp70 – Hsp70-like NBD/SBD; HEAT – HEAT-like helical repeats; ZnR – zinc ribbon domain; PYD – pyrin/CARD-like domain; SPB – SmpB-like domain; RTL – RNase toxin-like domain; HEPN – HEPN family nuclease domain; OB – OB-fold domain; iPD-D/ExK – inactivated PD-D/ExK fold; REC – Phosphoacceptor receiver-like domain; PLD – Phospholipase D-like nuclease domain; Vsr – very-short-patch-repair PD-D/ExK nuclease-like domain. Underneath each gene is a proposed protein name, with Cnu as an abbreviation for CoCoNuT.

225 CoCoNuT systems are extremely diverse and represented in a wide variety of bacteria,
226 particularly Pseudomonadota and Bacillota, but are nearly absent in archaea (Figure 4).

227

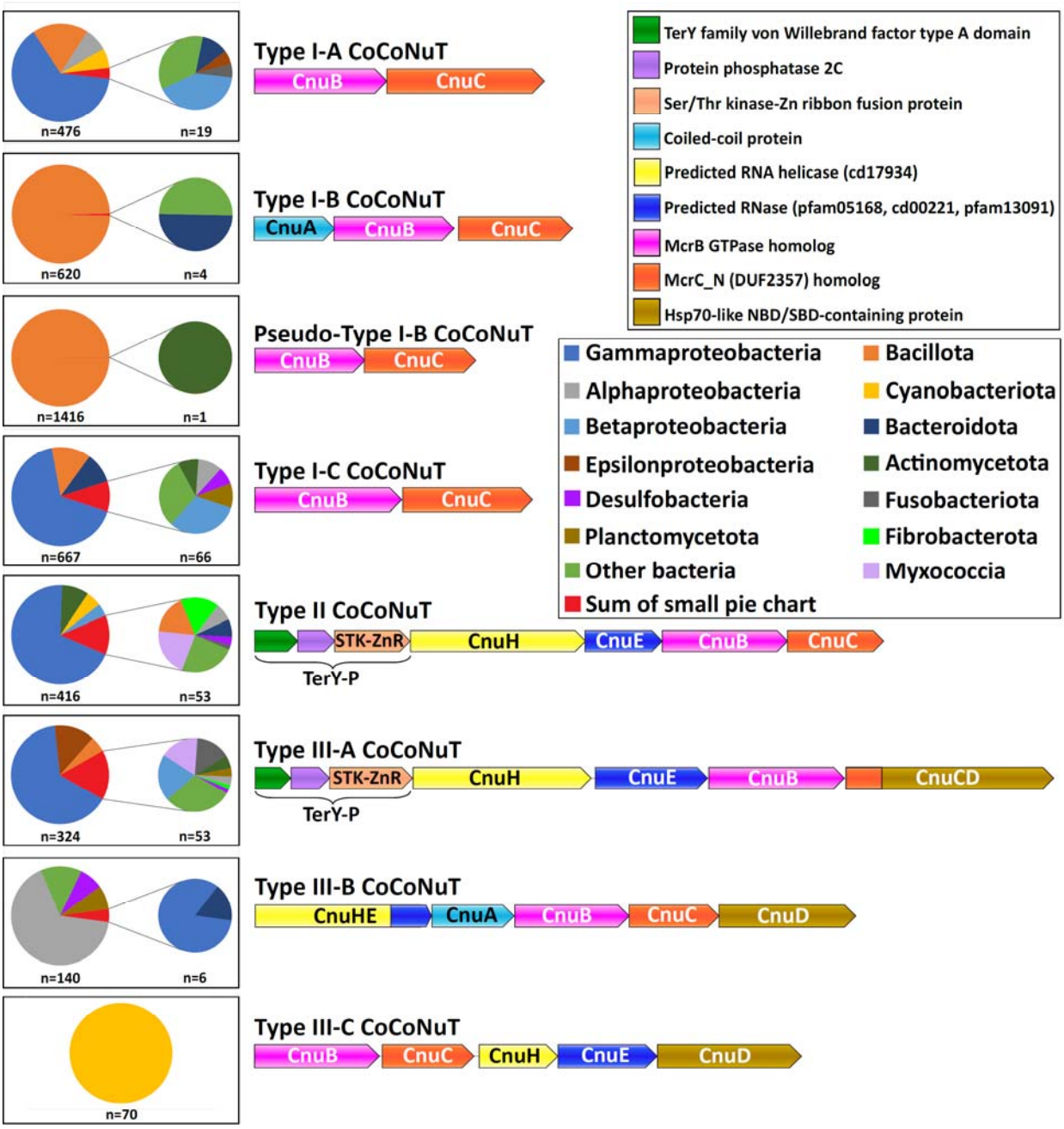

228

229 **Figure 4: Phyletic distribution of CoCoNuTs**

230 The phyletic distribution of CnuB/McrB GTPases in CoCoNuT systems found in genomic islands with distinct
231 domain compositions. Most CoCoNuTs are found in either Bacillota or Pseudomonadota, with particular
232 abundance in Gammaproteobacteria. Type I-B and the related Pseudo-Type I-B CoCoNuTs are restricted mainly to

233 Bacillota. In contrast, the other types are more common in Pseudomonadota, but can be found in a wide variety of
234 bacteria. Type III-B and III-C are primarily found in Alphaproteobacteria and Cyanobacteriota, respectively.

235

236 *Type I CoCoNuT systems*

237 We classified the CoCoNuTs into 3 types and 7 subtypes based on the GTPase domain
238 phylogeny and conserved genomic context (Figure 3). Type I-A and Type I-C systems consist of
239 McrB and McrC homologs only, which we denote CnuB and CnuC (Figure 3, Figure 5). Type I-B
240 systems usually encode a separate coiled-coil protein, which we denote CnuA, in addition to
241 CnuB/McrB and CnuC/McrC, with no coiled-coil fused to the McrB-like GTPase domain in CnuB
242 (Figure 3, Figure 5). CnuA is fused at the N-terminus to a pyrin (PYD)/CARD (caspase activation
243 and recruitment domain)-like helical domain and at the C-terminus to a phosphoacceptor
244 receiver (REC) domain (Figure 5, Supplementary Table S1). The association of the PYD/CARD-
245 like domains with CoCoNuTs suggests involvement in a programmed cell death (PCD)/abortive
246 infection-type response, as they belong to the DEATH domain superfamily and are best
247 characterized in the context of innate immunity, inflammasome formation, and PCD (Park et al.,
248 2007). The REC domains constitute one of the components of two-component regulatory
249 systems. They are targeted for phosphorylation by histidine kinases (Stock et al., 2000), which
250 could be a mechanism of Type I-B CoCoNuT regulation.

251 In contrast to Type II and Type III CnuB homologs, which contain only coiled-coils fused
252 at their N-termini (Figure 6), cold-shock domain (CSD)-like OB-folds are usually fused at the N-
253 termini of Type I CoCoNuT CnuB/McrB proteins, in addition to the coiled-coils (except for the
254 majority of Type I-B, where the coiled-coils are encoded separately) (Figure 5, Supplementary
255 Table S1) (Amir et al., 2018). Often, in Type I-B and I-C, but not Type I-A, a YTH-like domain, a
256 member of the modified base-binding EVE superfamily, is present in CnuB as well, between the
257 CSD and coiled-coil, or in Type I-B, between the CSD and the GTPase domain (Figure 5,
258 Supplementary Table S1) (Bell et al., 2020, Hazra et al., 2019, Liao et al., 2018).

259 The CnuC/McrC proteins in Type I CoCoNuTs, as well as those in Type II and Type III-B
260 and III-C, all contain an immunoglobulin-like N-terminal beta-sandwich domain of unknown
261 function, not present in the *E. coli* K-12 McrC homolog, similar to a wide range of folds from this
262 superfamily with diverse roles (Figure 5, Supplementary Table S1) (Natarajan et al., 2015,
263 Halaby et al., 1999). It is also present in non-CoCoNuT McrC homologs associated with McrB
264 GTPase homologs in the NxD clade, implying its function is not specific to the CoCoNuTs. In the
265 Type I-B and I-C CoCoNuT CnuC homologs, these domains most closely resemble Rho GDP-
266 dissociation inhibitor 1, suggesting that they may be involved in regulation of CnuB/McrB
267 GTPase activity (Dovas and Couchman, 2005).

268

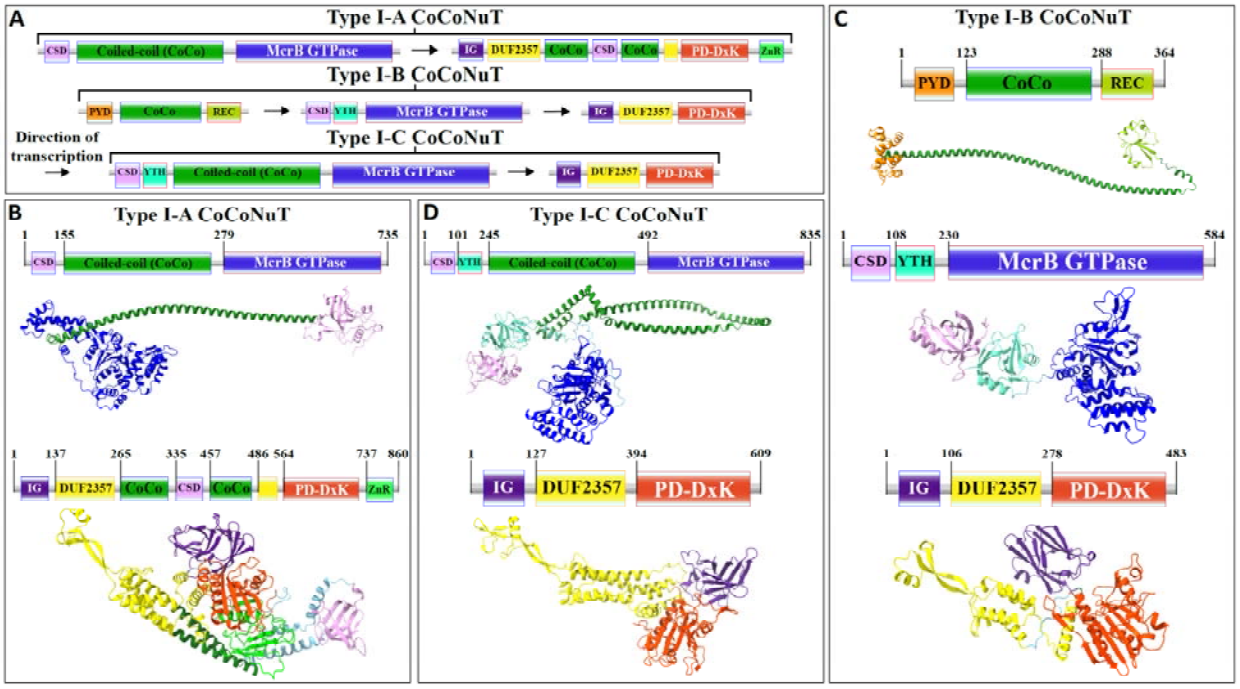

Figure 5: Domain composition, operon organization, and AlphaFold2 structural predictions of components of the Type I CoCoNuT systems

A) Type I CoCoNuT domain composition and operon organization. The arrows indicate the direction of transcription. B-D) High quality (Average pLDDT > 80), representative AlphaFold2 structural predictions for protein monomers in B) Type I-A CoCoNuT systems (CnuB and CnuC, from top to bottom), C) Type I-B CoCoNuT systems (CnuA, CnuB, and CnuC, from top to bottom), and D) Type I-C CoCoNuT systems (CnuB and CnuC, from top to bottom). Models were generated from representative sequences with the following GenBank accessions (see Supplementary Data for sequences and locus tags): ROR86958.1 (Type I-A CnuB), APL73566.1 (Type I-A CnuC), TKH01449.1 (Type I-B CnuA), GED20858.1 (Type I-B CnuB), GED20857.1 (Type I-B CnuC), GFD85286.1 (Type I-C CnuB), MBV0932851.1 (Type I-C CnuC). Abbreviations of domains: CSD – cold shock domain; YTH – YTH-like domain; CoCo – coiled-coil; IG – Immunoglobulin (IG)-like beta-sandwich domain; ZnR – zinc ribbon domain; PYD – pyrin/CARD-like domain; REC – Phosphoacceptor receiver-like domain. These structures were visualized with ChimeraX (Pettersen et al., 2021).

We also detected a close relative of Type I-B CoCoNuT in many *Bacillus* species, which we denoted Pseudo-Type I-B CoCoNuT because it lost the separate coiled-coil protein CnuA. Pseudo-Type I-B CoCoNuT occurs in genomic contexts suggesting a role in overcrowding-induced stress responses (Figure 3, Supplementary Figure S4).

Type II and III CoCoNuT systems

Type II and III CoCoNuT CnuB/McrB GTPase domains branch from within Type I-A and are encoded in a nearly completely conserved genomic association with a Superfamily 1 (SF1)

292 helicase of the UPF1-like clade, which we denote CnuH (Figure 3, Supplementary Table S1)
293 (Gorbalenya and Koonin, 1993, Fairman-Williams et al., 2010). The UPF1-like family
294 encompasses helicases with diverse functions acting on RNA and single-stranded DNA (ssDNA)
295 substrates, and notably, the prototypical UPF1 RNA helicase and its closest relatives are highly
296 conserved in eukaryotes, where they play a critical role in the nonsense-mediated decay (NMD)
297 RNA surveillance pathway (Cheng et al., 2007, Chakrabarti et al., 2011).

298 SF1 helicases are composed of two RecA-like domains which together harbor a series of
299 signature motifs required for the ATPase and helicase activities, including the Walker A and
300 Walker B motifs conserved in P-loop NTPases, which are located in the N-terminal RecA-like
301 domain (Fairman-Williams et al., 2010). In all 4 Type II and Type III CoCoNuT subtypes, following
302 the Walker A motif, the CnuH helicases contain a large helical insertion, with some of the
303 helices predicted to form coiled-coils (Figure 6). The Type II, Type III-A, and Type III-B CoCoNuT
304 CnuH helicases contain an OB-fold domain that, in Type II and Type III-A, is flanked by helices
305 predicted to form a stalk-like helical extension of the N-terminal RecA-like domain, a structural
306 feature characteristic of the entire UPF1/DNA2-like helicase family within SF1 (Chakrabarti et
307 al., 2011, Zhou et al., 2015, Kalathiya et al., 2019) (Figure 6). DALI comparisons show that the
308 CnuH predicted OB-fold domain in Type II CoCoNuTs is similar to the OB-fold domain in UPF1
309 and related RNA helicases SMUBP-2 and SEN1, and this holds for Type III-A as well, although, in
310 these systems, the best DALI hits are to translation factor components such as EF-Tu domain II
311 (Supplementary Table S1) (Chakrabarti et al., 2011, Morse et al., 2020). The Type III-B CnuH
312 predicted OB-folds also match that of UPF1, albeit with lower statistical support
313 (Supplementary Table S1).

314 In Type II and Type III-A CoCoNuTs, CnuH is fused at the N-terminus to a second OB-fold
315 domain similar to that of SmpB (small protein B) (Figure 6, Supplementary Figure S5,
316 Supplementary Table S1), which we denote SPB (SmpB-like). SmpB binds to SsrA RNA, also
317 known as transfer-messenger RNA (tmRNA), and is required for tmRNA to rescue stalled
318 ribosomes, via entry into their A-sites with its alanine-charged tRNA-like domain (Barends et al.,
319 2001, Himeno et al., 2014, Guyomar et al., 2021). The SPB domain is around 20 amino acids
320 shorter on average than SmpB itself, and a helix that is conserved in SmpB orthologs and
321 interacts with the tmRNA is absent in the CoCoNuT OB folds (Supplementary Figure S5) (Bessho
322 et al., 2007). However, two other structural elements of SmpB involved in binding tmRNA are
323 present (Supplementary Figure S5) (Gutmann et al., 2003). The N-terminal OB-folds in Type II
324 and III-A CnuH homologs also resemble prokaryotic HIRAN domains, which are uncharacterized,
325 but have eukaryotic homologs fused to helicases that bind ssDNA (Supplementary Figure S5)
326 (Chavez et al., 2018). These HIRAN domains, however, do not overlay with the CoCoNuT
327 domains any better than SmpB (Supplementary Figure S5), lack a small helix that SmpB and the
328 CoCoNuT domains share, and likely being DNA-binding, do not fit the other pieces of evidence
329 we gathered that all suggest an RNA-binding role for this domain in the CoCoNuTs (see below).

330 The Type II and Type III-A CoCoNuT CnuH helicases contain an additional domain,
331 structurally similar to the RelE/Colicin D RNase fold (Gucinski et al., 2019), which we denote
332 RNase toxin-like (RTL), located between the SPB OB-fold and the helicase (Figure 6,
333 Supplementary Table S1). The proteins of this family are ribosome-dependent toxins that cleave
334 either mRNA or tRNA in the ribosomal A-site (Pedersen et al., 2003). This domain was identified
335 by structural similarity search with the AF2 models, but no sequence conservation with
336 characterized members of this family was detected, leaving it uncertain whether the RTL
337 domain is an active nuclease. However, considerable divergence in sequence is not unusual in
338 this toxin family (Guglielmini and Van Melderen, 2011, Goeders et al., 2013). In Type III-B
339 CoCoNuTs, a wHTH domain resembling the archaeal ssDNA-binding protein Sul7s is fused to the
340 CnuH N-termini (Figure 6, Supplementary Table S1).

341 We searched for additional homologs of CnuH (see Methods). Our observations of the
342 contextual associations, both of the CoCoNuTs and their relatives, showed that helicases of this
343 large family are typically encoded in operons with downstream genes coding for an elongated
344 wHTH domain fused at its C-terminus to a variety of effectors, generally, nucleases, which we
345 denote CnuE (Figure 3, Figure 6). In the CoCoNuTs, except for Types III-B and III-C, these CnuE
346 effectors are HEPN ribonucleases, with one HEPN domain in Type II and two in Type III-A (Figure
347 6, Supplementary Table S1). In Type III-B, the effector is a Vsr (very-short-patch repair)-like PD-
348 (D/E)xK family endonuclease (Tsutakawa et al., 1999) fused directly to the helicase, with no
349 wHTH domain present, whereas in Type III-C, a distorted version of the elongated wHTH
350 domain is fused to two Phospholipase D (PLD) family endonuclease domains (Figure 6,
351 Supplementary Table S1). All these nucleases can degrade RNA, and some, such as HEPN, have
352 been found to cleave RNA exclusively (Pillon et al., 2021, Ipsaro et al., 2012, Mendez et al.,
353 2018, Laganeckas et al., 2011, Songailiene et al., 2020). We also detected coiled-coils in the
354 region between the wHTH and effector domains in Type II, Type III-A, and Type III-C CoCoNuT
355 CnuE homologs. Multimer structural modeling with AlphaFold2 suggests that the wHTH domain
356 in CnuE might interact with the coiled-coil-containing helical insertion of CnuH, perhaps
357 mediated by the coiled-coils in each protein, to couple the ATP-driven helicase activity to the
358 various nuclease effectors (Supplementary Figure S7). The accuracy of this model
359 notwithstanding, the fusion of the Vsr-like effector to CnuH in Type III-B CoCoNuTs and the
360 similarity of this system to the other CoCoNuT types strongly suggests that the CnuE effector
361 proteins in these systems form complexes with their respective CnuH helicases. An additional
362 factor in potential complexing by these proteins is the presence of coiled-coils in the associated
363 CnuB/McrB and CnuC/McrC homologs, which may interact with the coiled-coils in CnuH and
364 CnuE. Type III-B CoCoNuTs also code for a separate coiled-coil protein, which we denote CnuA,
365 as it resembles the CnuA protein encoded in Type I-B CoCoNuTs (Figure 3, Figure 5, Figure 6).
366 However, it is distinguished from Type I-B CnuA in containing no recognizable domains other
367 than the coiled-coil (Figure 3, Figure 5, Figure 6). This also could potentially interact with other
368 coiled-coil proteins in the system.

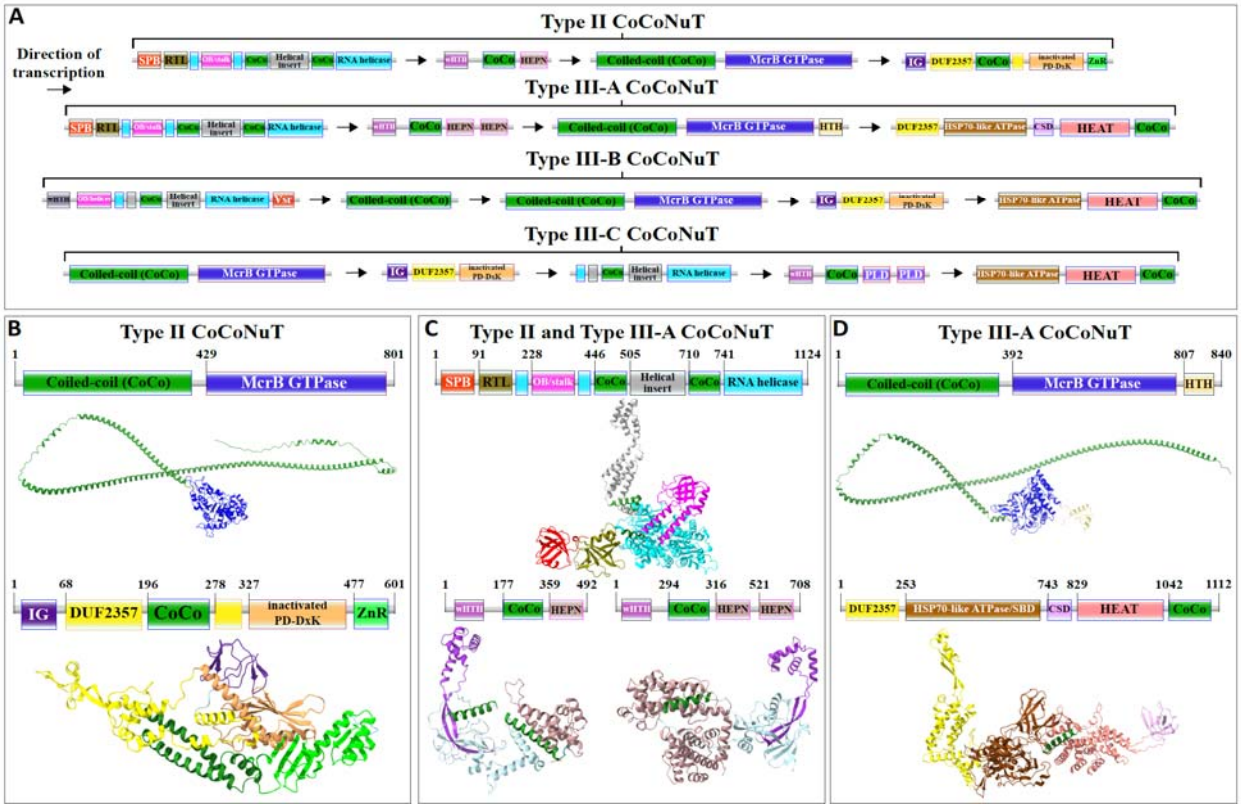

Figure 6: Domain composition, operon organization, and AlphaFold2 structural predictions for core protein components of Type II and III CoCoNuT systems

A) Type II and III CoCoNuT domain composition and operon organization. The arrows indicate the direction of transcription. Type II and III-A systems very frequently contain TerY-P systems as well, but not invariably, and these are never found in Type III-B or III-C, thus, we do not consider them core components. B-D) High quality (Average pLDDT > 80), representative AlphaFold2 structural predictions for protein monomers in B) Type II CoCoNuT systems (CnuB and CnuC, from top to bottom), C) Type II and III-A CoCoNuT systems (CnuH at the top, Type II CnuE on the bottom left, Type III-A CnuE on the bottom right), and D) Type III-A CoCoNuT systems (CnuB and CnuC, from top to bottom). Models were generated from representative sequences with the following GenBank accessions (see Supplementary Data for sequences and locus tags): AMO81401.1 (Type II CnuB), AVE71177.1 (Type II CnuC), AMO81399.1 (Type II and III-A CoCoNuT CnuH), AVE71179.1 (Type II CnuE), ATV59464.1 (Type III-A CnuE), PNG83940.1 (Type III-A CnuB), NMY00740.1 (Type III-A CnuC). Abbreviations of domains: CSD – cold shock domain; CoCo – coiled-coil; IG – Immunoglobulin (IG)-like beta-sandwich domain; ZnR – zinc ribbon domain; SPB – SmpB-like domain; RTL – RNase toxin-like domain; HEPN – HEPN family nuclease domain; OB/stalk – OB-fold domain attached to a helical stalk-like extension of ATPase; Vsr – very-short-patch-repair PD-D/ExK nuclease-like domain; PLD – Phospholipase D family nuclease domain; HEAT – HEAT-like helical repeats. These structures were visualized with ChimeraX (Pettersen et al., 2021).

Type II and Type III-A CoCoNuTs, the most widespread varieties apart from Type I, also include conserved genes coding for a "TerY-P" triad. TerY-P consists of a TerY-like von Willebrand factor type A (VWA) domain, a protein phosphatase 2C-like enzyme, and a serine/threonine kinase (STK) fused at the C-terminus to a zinc ribbon (Figure 3, Figure 6,

392 Supplementary Table S1). TerY-P triads are involved in tellurite resistance, associated with
393 various predicted DNA restriction and processing systems, and are predicted to function as a
394 metal-sensing phosphorylation-dependent signaling switch (Anantharaman et al., 2012). In
395 addition, TerY-P-like modules, in which the kinase is fused at the C-terminus to an OB-fold
396 rather than a zinc ribbon, have been recently shown to function as stand-alone antiphage
397 defense systems (Gao et al., 2020). The OB-fold fusion suggests that this kinase interacts with
398 an oligonucleotide and raises the possibility that the zinc ribbon, which occupies the same
399 position in the CoCoNuTs, is also nucleic acid-binding. Almost all CoCoNuT systems containing
400 *cnuHE* operons also encompass TerY-P, with a few exceptions among Terrabacterial Type II
401 systems and Myxococcal Type III-A systems, implying an important contribution to their
402 function (Supplementary Data). However, the complete absence of the TerY-P module in Type
403 III-B and Type III-C systems implies that when different nucleases and other putative effectors
404 fused to the helicase are present, TerY-P is dispensable for the CoCoNuT activity. Therefore, we
405 do not consider them to be core components of these systems.

406 Type II and Type III-A CoCoNuTs have similar domain compositions, but a more detailed
407 comparison reveals substantial differences. The CnuE proteins in Type II contain one HEPN
408 domain with the typical RxxxxH RNase motif conserved in most cases, whereas those in Type III-
409 A contain two HEPN domains, one with the RxxxxH motif, and the other, closest to the C-
410 terminus, with a shortened RxH motif. Furthermore, Type III-A CnuB/McrB GTPase homologs
411 often contain C-terminal HTH-domain fusions absent in Type II (Figure 6). Finally, striking
412 divergence has occurred between the Type II and III-A CnuC/McrC homologs. Type II CnuCs
413 resemble Type I-A CnuCs, which contain N-terminal immunoglobulin-like beta-sandwich
414 domains, PD-D/ExK nucleases, zinc ribbon domains, and insertions into DUF2357 containing
415 coiled-coils and a CSD-like OBD. However, in Type II CnuCs, this domain architecture underwent
416 reductive evolution (Figure 5, Figure 6, Supplementary Table S1). In particular, the beta-
417 sandwich domain and coiled-coils are shorter, the CSD was lost, the nuclease domain was
418 inactivated, and in many cases, the number of Zn-binding CPxC motifs was reduced from three
419 to two (Figure 5, Figure 6, Supplementary Table S1). This degeneration pattern could indicate
420 functional replacement by the associated CnuH and CnuE proteins, often encoded in reading
421 frames overlapping with the start of the *cnuBC* operon.

422 By contrast, Type III-A CnuC/McrC homologs entirely lost the beta-sandwich domain,
423 PD-D/ExK nuclease, and zinc ribbon found in Type I-A and Type II, but gained an Hsp70-like
424 NBD/SBD unit similar to those that are fused to the McrB GTPase in early branching members
425 of the NxD clade. They have also acquired a helical domain similar to the HEAT repeat family,
426 and in some cases, a second CSD (Figure 3, Figure 5, Figure 6, Supplementary Table S1). Most
427 Type III-A CnuCs contain a CSD and coiled-coils, and thus, resemble Type I-A, but the positioning
428 of these domains, which in Type I-A are inserted into the DUF2357 helix bundle, is not
429 conserved in Type III-A, where these domains are located outside DUF2357 (Figure 5, Figure 6).

430 Hsp70-like ATPase NBD/SBD domains and HEAT-like repeats are fused to the CnuC/McrC
431 N-terminal DUF2357 domain in Type III-A CoCoNuT, but their homologs in Type III-B and III-C
432 are encoded by a separate gene. We denote these proteins CnuD and CnuCD, the latter for the
433 CnuC-CnuD fusions in Type III-A. The separation of these domains in Type III-B and III-C implies
434 that fusion is not required for their functional interaction with the CnuBC/McrBC systems
435 (Figure 6 A, Supplementary Table S1). CnuD proteins associated with both Type III-B and III-C
436 contain predicted coiled-coils, suggesting that they might interact with the large coiled-coil in
437 the CnuB homologs (Figure 6 A).

438 In the CnuD homologs found in the CoCoNuTs and fused to NxD McrB GTPases, Walker
439 B-like motifs (Yamamoto et al., 2014) are usually, but not invariably, conserved, whereas the
440 sequences of the helical domains adjacent to the motifs are more strongly constrained. Walker
441 A-like motifs (Chang et al., 2008) are present but degenerate (Supplementary Figure S8).
442 Therefore, it appears likely that the CoCoNuT CnuD homologs bind ATP/ADP but hydrolyze ATP
443 with extremely low efficiency, at best. Such properties in an Hsp70-like domain are better
444 compatible with RNA binding than unfolded protein binding or remodeling, suggesting that
445 these CnuD homologs may target the respective systems to aberrant RNA. Many Hsp70
446 homologs have been reported to associate with ribosomes (Mayer, 2021, Willmund et al.,
447 2013), which could also be true for the CoCoNuT Cnu(C)Ds.

448 Consistent with this prediction, Type II and III-A CoCoNuTs likely target RNA rather than
449 DNA, given that the respective operons encode HEPN RNases, typically the only recognizable
450 nuclease in these systems. All CnuC/McrC homologs in Type II or III CoCoNuT systems lack the
451 PD-D/ExK catalytic motif that is required for nuclease activity, although for Type II and Type III-B
452 and III-C, but not Type III-A, structural modeling indicates that the inactivated nuclease domain
453 was retained, likely for a nucleic acid-binding role (Figure 6, Supplementary Table S1). In Type
454 III-A CoCoNuT, the nuclease domain was lost entirely and replaced by the Hsp70-like NBD/SBD
455 domain with RNA-binding potential described above (Figure 6, Supplementary Table S1). Often,
456 one or two CSDs, generally RNA-binding domains, although capable of binding ssDNA, are fused
457 to Type III-A CnuC homologs as well (Figure 6, Supplementary Table S1) (Heinemann and Roske,
458 2021). RNA targeting capability of Type III-B and III-C can perhaps be inferred from their
459 similarity to Type III-A in encoding CnuD Hsp70-like proteins. Moreover, higher-order
460 associations of Type II and Type III-A CoCoNuT systems with various DNA restriction systems
461 suggest a two-pronged DNA and RNA restriction strategy reminiscent of Type III CRISPR-Cas
462 (see below).

463 We suspect that RNA targeting is an ancestral feature of the CoCoNuT systems. Several
464 observations are compatible with this hypothesis:

465 1) Most of the CoCoNuTs encompass HEPN nucleases that appear to possess exclusive
466 specificity for RNA.

467 2) CSD-like OB-folds are pervasive in these systems, being present in the CnuB/McrB
468 homologs of all Type I subtypes and in Type I-A and Type III-A CnuC/McrC homologs. As
469 previously noted, these domains typically bind RNA, although they could bind ssDNA as well.

470 3 YTH-like domains are present in most Type I CoCoNuts, particularly, in almost all early
471 branching Type I-B and I-C systems, suggesting that the common ancestor of the CoCoNuTs
472 contained such a domain. YTH domains in eukaryotes sense internal N6-methyladenosine
473 (m6A) in mRNA (Hazra et al., 2019, Liao et al., 2018, Patil et al., 2018).

474 4) Type II and Type III-B/III-C CoCoNuTs, which likely target RNA, given the presence of
475 HEPN domains and Hsp70 NBD/SBD homologs, retain inactivated PD-DxK nuclease domains,
476 suggesting that these domains contribute an affinity for RNA inherited from Type I-A CoCoNuTs.
477 PD-(D/E)xK nucleases are generally DNA-specific, however, some examples of RNase activity
478 have been reported (Mendez et al., 2018, Laganeckas et al., 2011). The inactivated PD-DxK
479 domains might also bind DNA from which the target RNA is transcribed.

480

481 *Complex higher-order associations between CoCoNuTs, CARF domains, and other*
482 *defense systems*

483 Genomic neighborhoods of many Type II and Type III-A CoCoNuTs encompass complex
484 operonic associations with genes encoding several types of CARF (CRISPR-Associated Rossmann
485 Fold) domain-containing proteins. This connection suggests multifarious regulation by cyclic
486 (oligo)nucleotide second messengers synthesized in response to viral infection and bound by
487 CARF domains (Makarova et al., 2020a, McMahon et al., 2020, Zhu et al., 2021). Activation of an
488 effector, most often a nuclease, such as HEPN or PD-(D/E)xK, by a CARF bound to a cyclic
489 (oligo)nucleotide is a crucial mechanism of CBASS (cyclic oligonucleotide-based antiphage
490 signaling system) as well as Type III CRISPR-Cas systems (McMahon et al., 2020, Makarova et al.,
491 2020a, Zhu et al., 2021). These CARF-regulated enzymes generally function as a fail-safe that
492 eventually induces PCD/dormancy when other antiphage defenses fail to bring the infection
493 under control and are deactivated, typically through cleavage of the second messenger by a
494 RING nuclease, if other mechanisms succeed (Makarova et al., 2012, Koonin and Zhang, 2017,
495 Makarova et al., 2020a, Koonin and Krupovic, 2019).

496 The presence of CARFs could implicate the HEPN domains of these systems as PCD
497 effectors that would carry out non-specific RNA degradation in response to infection.
498 Surprisingly, however, most of these CARF domain-containing proteins showed the highest
499 similarity to RtcR, a sigma54 transcriptional coactivator of the RNA repair system RtcAB with a
500 CARF-ATPase-HTH domain architecture, suggesting an alternative functional prediction
501 (Supplementary Figure S9, Supplementary Table S1). Specifically, by analogy with RtcR,
502 CoCoNuT-associated CARF domain-containing proteins might bind (t)RNA fragments with 2',3'
503 cyclic phosphate ends (Kotta-Loizou et al., 2022, Hughes et al., 2020). This interaction could
504 promote transcription of downstream genes, in this case, genes encoding CoCoNuT

505 components, through binding an upstream activating sequence by the HTH domain fused to the
506 CARF-ATPase C-terminus (Hughes et al., 2020, Kotta-Loizou et al., 2022).

507 The manifold biological effects of tRNA-like fragments are only beginning to be
508 appreciated. Lately, it has been shown that bacterial anticodon nucleases, in response to
509 infection and DNA degradation by phages, generate tRNA fragments, likely a signal of infection
510 and a defensive strategy to slow down the translation of viral mRNA, and that phages can
511 deploy tRNA repair enzymes and other strategies to counteract this defense mechanism (Bitton
512 et al., 2015, van den Berg et al., 2023, Kaufmann, 2000, Ishita et al., 2021). Moreover, the
513 activity of the HEPN ribonucleases in the CoCoNuTs themselves would produce RNA cleavage
514 products with cyclic phosphate ends that might be bound by the associated RtcR-like CARFs
515 (Shigematsu et al., 2018, Pillon et al., 2021), in a potential feedback loop.

516 Such a CoCoNuT mechanism could complement the function of RtcAB, as RtcA is an RNA
517 cyclase that converts 3′-phosphate RNA termini to 2′,3′-cyclic phosphate and thus, in a
518 feedback loop, generates 2',3'-cyclic phosphate RNA fragments that induce expression of the
519 operon (Genschik et al., 1998, Das and Shuman, 2013, Hughes et al., 2020). Acting downstream
520 of RtcA, RtcB is an RNA ligase that joins 2',3'-cyclic phosphate RNA termini to 5'-OH RNA
521 fragments, generating a 5'-3' bond and, in many cases, reconstituting a functional tRNA (Tanaka
522 and Shuman, 2011). Recent work has shown that, in bacteria, the most frequent target of RtcB
523 is SsrA, the tmRNA (Kotta-Loizou et al., 2022). Intriguingly, as described above, in order to
524 rescue stalled ribosomes, tmRNA must bind to SmpB, an OB-fold protein highly similar to the
525 predicted structures of the SPB domains fused at the N-termini of the Type II and III-A
526 CoCoNuTs, which are the only types that frequently associate with RtcR homologs
527 (Supplementary Figure S9, Figure 7) (Himeno et al., 2014, Guyomar et al., 2021).

528 There are notable parallels between CoCoNuTs and Type III CRISPR-Cas systems, where
529 the Cas10-Csm-crRNA effector complex binds phage RNA complementary to the spacer of the
530 crRNA, triggering both restriction of phage DNA and indiscriminate cleavage of RNA (McMahon
531 et al., 2020). The target RNA recognition stimulates the production of cyclic oligoadenylate
532 (cOA) signals by Cas10, which activate, via CARF domain binding, PCD effectors, typically HEPN
533 domain-containing proteins, such as Csm6, that function as promiscuous RNases (Pillon et al.,
534 2021, Millman et al., 2020). One of the two outcomes can result from this cascade: the
535 infection can either be eradicated quickly due to the restriction of the virus DNA, which inhibits
536 cOA signaling via the depletion of viral RNA, along with the activity of RING nucleases, thus
537 averting PCD, or the continued presence of viral RNA stimulates cOA signaling until PCD or
538 dormancy occurs, limiting the spread of viruses to neighboring cells in the bacterial population
539 (Makarova et al., 2012, Koonin and Aravind, 2002, Koonin and Krupovic, 2019).

540 If CoCoNuTs associated with RtcR homologs can induce PCD, a conceptually similar but
541 mechanistically distinct phenomenon might occur. Although many of these CoCoNuTs only
542 contain an appended gene encoding a CARF domain-containing protein at the 5' end of the
543 predicted operon (Supplementary Figure S9), there are also numerous cases where several

544 types of DNA restriction systems are encoded between the CARF gene and the CoCoNuT (Figure
545 7). In these cases, nearly all genes are in an apparent operonic organization that can extend
546 upwards of 40 kb (Figure 7). Although internal RtcR-independent promoters likely exist in these
547 large loci, the consistent directionality and close spacing of the genes in these superoperons
548 suggests coordination of expression. The complex organization of the CARF-CoCoNuT genomic
549 regions, and by implication, the corresponding defense mechanisms, might accomplish the
550 same effect as Type III CRISPR-Cas, contriving a no-win situation for the target virus. Under this
551 scenario, the virus is either destroyed by the activity of the DNA restriction systems, which
552 would inhibit signal production (likely RNA fragments with cyclic phosphate ends rather than
553 cOA) and drive down CoCoNuT transcription, thereby preventing PCD, or as the virus replicates,
554 signaling and CoCoNuT transcription would continue until the infection is aborted by PCD or
555 dormancy caused by the degradation of host mRNA via the HEPN RNase(s) of the CoCoNuT.

556 In many species of *Pseudomonas*, where CoCoNuTs are almost always associated with
557 RtcR and various ancillary factors, Type I RM systems often contain an additional gene that
558 encodes a transmembrane helix and a long coiled-coil fused to an RmuC-like nuclease (Figure
559 7). These proteins were recently described as ShdA, the core component of the *Pseudomonas*-
560 specific defense system Shield (Macdonald et al., 2022). These can potentially interact with
561 coiled-coils in the CoCoNuTs, perhaps, guiding them to the DNA from which RNA targeted by
562 the CoCoNuTs is being transcribed, or vice versa (Figure 7).

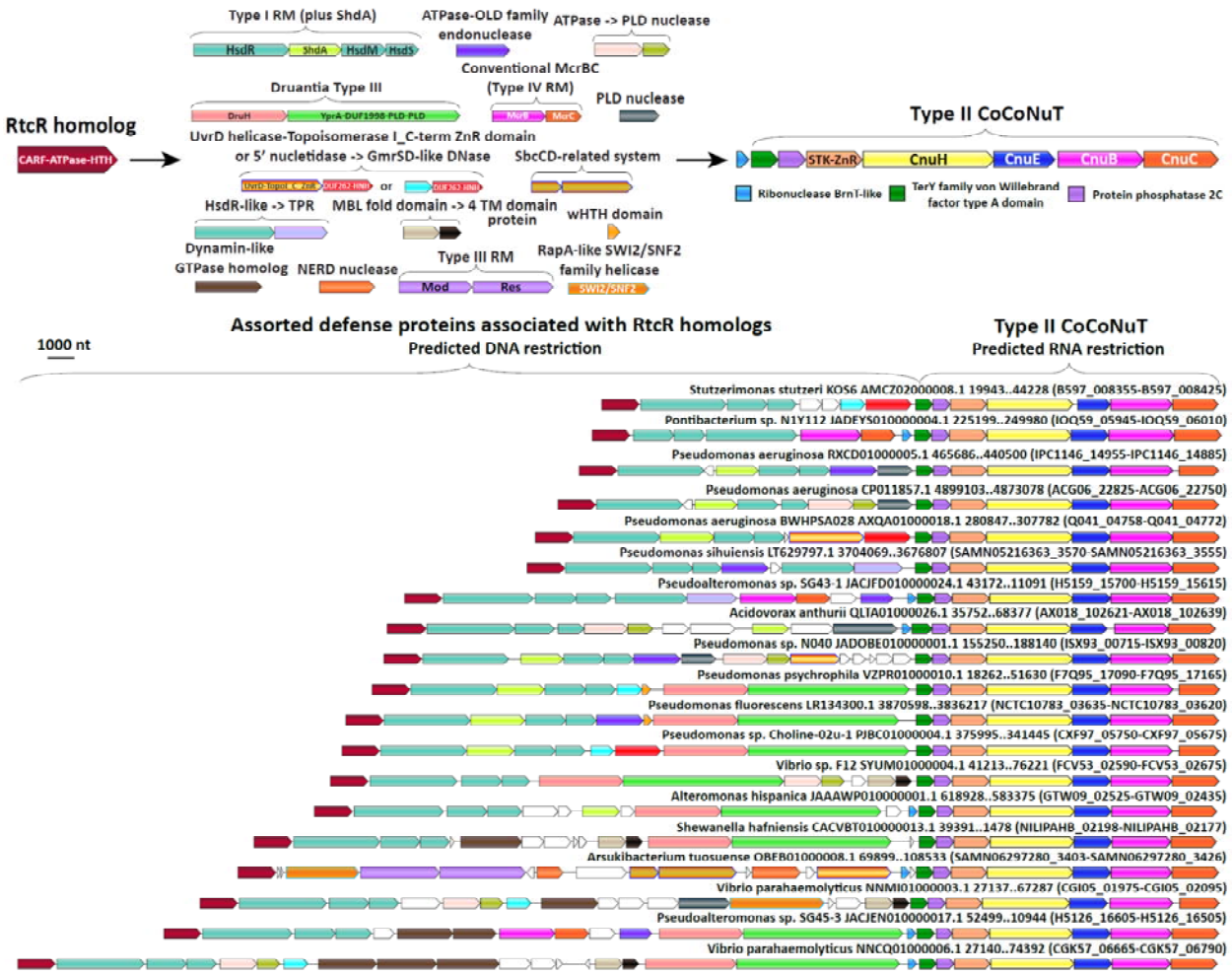

Figure 7: Complex operonic associations of Type II CoCoNuTs

Type II CoCoNuTs are frequently associated with RtcR homologs, and in many cases, ancillary defense genes are located between the RtcR gene and the CoCoNuT, almost always oriented in the same direction in an apparent superoperon. Abbreviations of domains: YprA – YprA-like helicase domain; DUF1998 - DUF1998 is often found in or associated with helicases and contains four conserved, putatively metal ion-binding cysteine residues; PLD – Phospholipase D family nuclease domain; SWI2/SNF2 – SWI2/SNF2-family ATPase; HsdR/M/S – Type I RM system restriction, methylation, and specificity factors; ShdA – Shield system core component ShdA; TPR – Tetratricopeptide repeat protein; MBL fold – Metallo-beta-lactamase fold; 4 TM domain – Protein with 4 predicted transmembrane helices; Mod/Res – Type III RM modification and restriction factors.

A notable difference between the generally similar, dual DNA and RNA-targeting mechanism of many Type III CRISPR-Cas systems and the proposed mechanism of the CoCoNuTs is that viral RNA recognition by the Cas10-Csm complex, rather than binding of a second messenger to a CARF domain, activates both DNA cleavage activity by the HD domain and production of cOA that triggers non-specific RNA cleavage. In contrast, in the CARF-containing CoCoNuTs, both the DNA and RNA restriction factors appear to be arranged such

580 that binding of a 2',3' cyclic phosphate RNA fragment by the CARF domain would initiate the
581 expression of the entire cluster (McMahon et al., 2020). In the case of the CoCoNuTs, signals of
582 infection could promote transcription, first of the DNA restriction systems, and then, the
583 CoCoNuT itself, a predicted RNA restriction system. In these complex configurations of the
584 CoCoNuT genome neighborhoods (Figure 7), the gene order is likely to be important, with Type
585 I RM almost always directly following CARF genes and CoCoNuTs typically coming last, although
586 Druantia Type III sometimes follows the CoCoNuT. As translation in bacteria is co-
587 transcriptional, the products of genes transcribed first would accumulate before those of the
588 genes transcribed last, so that the full, potentially suicidal impact of the CoCoNuT predicted
589 RNA nucleolytic engine would only be felt after the associated DNA restriction systems had
590 ample time to act – and possibly, fail (Irastortza-Olaziregi and Amster-Choder, 2020).

591

592 Concluding remarks

593 In recent years, systematic searches for defense systems in prokaryotes, primarily by
594 analysis of defense islands, revealed enormous, previously unsuspected diversity of such
595 systems that function through a remarkable variety of molecular mechanisms. In this work, we
596 uncovered the hidden diversity and striking hierarchical complexity of a distinct class of defense
597 mechanisms, the Type IV (McrBC) restriction systems. We then zeroed in on a single major but
598 previously overlooked branch of the McrBC systems, which we denoted CoCoNuTs for their
599 salient features, namely, the presence of extensive coiled-coil structures and tandem nucleases.
600 Astounding complexity was discovered at this level as well, with 3 distinct types and multiple
601 subtypes of CoCoNuTs that differ by their domain compositions and genomic associations. All
602 CoCoNuTs contain domains capable of interacting with translation systems components, such
603 as the SmpB-like OB-fold, Hsp70 homologs, or YTH domains, along with RNases, such as HEPN,
604 suggesting that at least one of the activities of these systems targets RNA. Most of the
605 CoCoNuTs are likely endowed with DNA-targeting activity as well, either by factors integral to
606 the system, such as the McrC nuclease, or more loosely associated, such as Type I RM and
607 Druantia Type III systems that are encoded in the same predicted superoperon with many
608 CoCoNuTs. Numerous CoCoNuTs are associated with proteins containing CARF domains,
609 suggesting that cyclic (oligo)nucleotides regulate the CoCoNuT activity. Given the presence of
610 the RtcR-like CARF domains, it appears likely that the specific second messengers involved are
611 RNA fragments with cyclic phosphate termini. We hypothesize that the CoCoNuTs, in
612 conjunction with ancillary restriction factors, implement an echeloned defense strategy
613 analogous to that of Type III CRISPR-Cas systems, whereby an immune response eliminating
614 virus DNA and/or RNA is launched first, but then, if it fails, an abortive infection response
615 leading to PCD/dormancy via host RNA cleavage takes over.

616

617 Methods

618 *Comprehensive identification and phylogenetic and genomic neighborhood analysis of*
619 *McrB and McrC proteins*

620 The comprehensive search for McrB and McrC proteins was seeded with publicly
621 available multiple sequence alignments COG1401 (McrB GTPase domain), AAA_5 (The branch
622 of AAA+ ATPases containing the McrB GTPase), COG4268 (McrC), PF10117 (McrBC), COG1700
623 (McrC PD-D/ExK nuclease domain), PF04411 (McrC PD-D/ExK nuclease domain), PF09823 (McrC
624 N-terminal DUF2357). Additional alignments and individual queries were derived from data
625 from our previous work on the EVE domain family (Bell et al., 2020). All alignments were
626 clustered, and each sub-alignment or individual query sequence was used to produce a
627 position-specific scoring matrix (PSSM). These PSSMs were used as PSI-BLAST queries against
628 the non-redundant (nr) NCBI database (*E*-value ≤ 10) (Altschul et al., 1997). Although a branch
629 of McrB GTPase homologs has been described in animals, these are highly divergent in function,
630 and no associated McrC homologs have been reported (Iyer et al., 2004). Therefore, we
631 excluded eukaryotic sequences from our analysis to focus on the composition and contextual
632 connections of prokaryotic McrBC systems. Genome neighborhoods for the hits were generated
633 by downloading their gene sequence, coordinates, and directional information from GenBank,
634 as well as for 10 genes on each side of the hit. Domains in these genes were identified using
635 PSI-BLAST against alignments of domains in the NCBI Conserved Domain Database (CDD) and
636 Pfam (*E*-value 0.001). Some genes were additionally analyzed with HHpred (Gabler et al., 2020).
637 Then, these neighborhoods were filtered for the presence of a COG1401 hit (McrB GTPase
638 domain), or hits to both an McrB "alias" (MoxR, AAA_5, COG4127, DUF4357, Smc, WEMBL,
639 Myosin_tail_1, DUF3578, EVE, Mrr_N, pfam01878) and an McrC "alias" (McrBC, McrC, PF09823,
640 DUF2357, COG1700, PDDEXK_7, RE_LlaJI). These aliases were determined from a preliminary
641 manual investigation of the data using HHpred (Zimmermann et al., 2018). Several of the McrB
642 aliases are not specific to McrB, and instead are domains commonly fused to McrB GTPase
643 homologs, or are larger families, such as AAA_5, that contain McrB homologs. We found that
644 many *bona fide* McrB homologs, validated by HHpred, produced hits not to COG1401 but rather
645 to these other domains, so we made an effort to retain them.
646 The McrB candidates identified by this filtering process were clustered to a similarity
647 threshold of 0.5 with MMseqs2 (Hauser et al., 2016), after which the sequences in each cluster
648 were aligned with MUSCLE (Edgar, 2004). Next, profile-to-profile similarity scores between all
649 clusters were calculated with HHsearch (Söding, 2004). Clusters with high similarity, defined as
650 a pairwise score to self-score ratio > 0.1, were aligned to each other with HHalign (Söding et
651 al., 2006). This procedure was performed for a total of 3 iterations. The alignments resulting
652 from this protocol were analyzed with HHpred to remove false positives, after which the
653 GTPase domain sequences were extracted manually using HHpred, and the alignments were
654 used as queries for a second round of PSI-BLAST against the nr NCBI database as described
655 above. At this stage, the abundance of the CoCoNuT and CoCoPALM (coiled-coil and pilus
656 assembly linked to McrBC, see below) types of McrB GTPases had become apparent, therefore,
657 results of targeted searches for these subtypes were included in the pool of hits from the
658 second round of PSI-BLAST. Genome neighborhoods were generated for these hits and filtered
659 for aliases as described above. Further filtering of the data, which did not pass this initial filter,
660 involved relaxing the criteria to include neighborhoods with only one hit to an McrB or McrC

661 alias, but with a gene adjacent to the hit (within 90 nucleotides), oriented in the same direction
662 as the hit, and encoding a protein of sufficient size (> 200 aa for McrB, > 150 aa for McrC) to be
663 the undetected McrB or McrC component. Afterward, we filtered the remaining data to retain
664 genome islands with no McrBC aliases but with PSI-BLAST hits in operonic association with
665 genes of sufficient size, as described above, to be the other McrBC component. These data,
666 which contained many false positives but captured many rare variants, were then clustered and
667 analyzed as described above to remove false positives. Next, an automated procedure was
668 developed to excise the GTPase domain sequences using the manual alignments generated
669 during the first phase of the search as a reference. These GTPase sequences were further
670 analyzed by clustering and HHpred to remove false positives. Definitive validation by pairing
671 McrB homologs with their respective McrC homologs was also used to corroborate their
672 identification. Occasionally, the McrB and McrC homologs were separated by intervening
673 genes, or the operon order was reversed, and consideration of those possibilities allowed the
674 validation of many additional systems. The pairing process was complicated by and drew our
675 attention to the frequent occurrence of multiple copies of McrBC systems in the same islands
676 that may function cooperatively. Finally, the rigorously validated set of McrBC pairs,
677 supplemented only with orphans manually annotated as McrBC components using HHpred,
678 were used for our phylogenetics. The final alignments of GTPase and DUF2357 domains were
679 produced using the iterative alignment procedure described above for 10 iterations.
680 Approximately-maximum-likelihood trees were built with the FastTree program (Price et al.,
681 2010) from representative sequences following clustering to a 0.9 similarity threshold with
682 MMseqs2. The phyletic distribution was calculated by assigning a weight to the lineage of each
683 sequence that was inversely proportional to its cluster size (1/n, where n=the cluster size).
684
685 *Preliminary phylogenetic analysis of CoCoNuT CnuH helicases*
686
687 A comprehensive search and phylogenetic analysis of this family was beyond the scope
688 of this work, but to determine the relationships between the CoCoNuTs and the rest of the
689 UPF1-like helicases, we used the following procedure. We retrieved the best 2000 hits in each
690 of two searches with UPF1 and CoCoNuT helicases as queries against both a database
691 containing predicted proteins from 24,757 completely sequenced prokaryotic genomes
692 downloaded from the NCBI GenBank in November 2021 and a database containing 72
693 representative eukaryotic genomes that were downloaded from the NCBI GenBank in June
694 2020. Next, we combined all proteins in four searches, made a nonredundant set, and
695 annotated them using CDD profiles, as described above. Then, we aligned them with MUSCLE
696 v5 (Robert, 2022), constructed an approximately-maximum-likelihood tree with FastTree, and
697 mapped the annotations onto the tree. Genome neighborhoods were generated for these hits,
698 as described above.

699 *Structural modeling with AlphaFold2 and searches for related folds*
700
701 Protein structures were predicted using AlphaFold2 (AF2) v2.2.0 with local installations
702 of complete databases required for AF2 (Jumper et al., 2021). Only protein models with

703 average predicted local distance difference test (pLDDT) scores ≥ 80 were retained for further
704 analysis (Mariani et al., 2013). Many of these models were used as queries to search for
705 structurally similar proteins using DALI v5 against the Protein Data Bank (PDB) and using
706 FoldSeek against the AlphaFold/UniProt50 v4, AlphaFold/Swiss-Prot v4, AlphaFold/Proteome
707 v4, and PDB100 2201222 databases (Holm, 2020, van Kempen et al., 2023). Structure
708 visualizations and comparisons were performed with ChimeraX (Pettersen et al., 2021) and the
709 RCSB PDB website (Berman et al., 2000).

710 **Data availability**

711 All data generated and analyzed in this study are included in the manuscript and
712 supporting files. The CoCoNuT systems are documented in detail in the Supplementary Data.
713 The AlphaFold2 structures generated and presented in the figures are available at
714 modelarchive.org with accessions available in Supplementary Table S2.

715 **Conflict of interest**

716 The authors declare no conflict of interest

717

718 **Author contributions**

719 R.T.B and E.V.K. initiated the project; R.T.B., Y.I.W., and E.V.K. designed research; R.T.B., H.S.,
720 and K.S.M. analyzed data; R.T.B and E.V.K. wrote the manuscript that was edited and approved
721 by all authors. The authors declare no competing interests.

722 **Acknowledgments**

723 The authors thank Becky Xu Hua Fu (University of California, San Francisco) for correspondence
724 that led to her contribution of the name CoCoNuT, Andrew Z. Fire and Usman Enam (Stanford
725 University) for critical reading of the manuscript and insightful comments, Joseph Bondy-
726 Denomy (University of California, San Francisco) for bringing the Shield factor ShdA to our
727 attention, and Koonin group members for helpful discussions. The authors' research is
728 supported by the Intramural Research Program of the National Institutes of Health (National
729 Library of Medicine).

730

731

732 References

733 AGRAWAL, N., DASARADHI, P. V., MOHMMED, A., MALHOTRA, P., BHATNAGAR, R. K. & MUKHERJEE, S.
734 K. 2003. RNA interference: biology, mechanism, and applications. *Microbiol Mol Biol Rev,* 67**,**
735 657-85.
736 ALTSCHUL, S. F., MADDEN, T. L., SCHÄFFER, A. A., ZHANG, J., ZHANG, Z., MILLER, W. & LIPMAN, D. J.
737 1997. Gapped BLAST and PSI-BLAST: a new generation of protein database search programs.
738 *Nucleic acids research,* 25**,** 3389-3402.
739 AMIR, M., KUMAR, V., DOHARE, R., ISLAM, A., AHMAD, F. & HASSAN, M. I. 2018. Sequence, structure
740 and evolutionary analysis of cold shock domain proteins, a member of OB fold family. *Journal of*
741 *Evolutionary Biology,* 31**,** 1903-1917.
742 ANANTHARAMAN, V., IYER, L. M. & ARAVIND, L. 2012. Ter-dependent stress response systems: novel
743 pathways related to metal sensing, production of a nucleoside-like metabolite, and DNA-
744 processing. *Molecular bioSystems,* 8**,** 3142-3165.
745 BARENDS, S., KARZAI, A. W., SAUER, R. T., WOWER, J. & KRAAL, B. 2001. Simultaneous and functional
746 binding of SmpB and EF-Tu-TP to the alanyl acceptor arm of tmRNA. *J Mol Biol,* 314**,** 9-21.
747 BELL, R. T., WOLF, Y. I. & KOONIN, E. V. 2020. Modified base-binding EVE and DCD domains: striking
748 diversity of genomic contexts in prokaryotes and predicted involvement in a variety of cellular
749 processes. *BMC Biol,* 18**,** 159.
750 BERMAN, H. M., WESTBROOK, J., FENG, Z., GILLILAND, G., BHAT, T. N., WEISSIG, H., SHINDYALOV, I. N. &
751 BOURNE, P. E. 2000. The Protein Data Bank. *Nucleic Acids Res,* 28**,** 235-42.
752 BESSHO, Y., SHIBATA, R., SEKINE, S.-I., MURAYAMA, K., HIGASHIJIMA, K., HORI-TAKEMOTO, C.,
753 SHIROUZU, M., KURAMITSU, S. & YOKOYAMA, S. 2007. Structural basis for functional mimicry of
754 long-variable-arm tRNA by transfer-messenger RNA. *Proceedings of the National Academy of*
755 *Sciences,* 104**,** 8293-8298.
756 BITTON, L., KLAIMAN, D. & KAUFMANN, G. 2015. Phage T4-induced DNA breaks activate a tRNA repair-
757 defying anticodon nuclease. *Mol Microbiol,* 97**,** 898-910.
758 BOURNE, H. R., SANDERS, D. A. & MCCORMICK, F. 1991. The GTPase superfamily: conserved structure
759 and molecular mechanism. *Nature,* 349**,** 117-27.
760 BURROUGHS, A. M., ZHANG, D., SCHÄFFER, D. E., IYER, L. M. & ARAVIND, L. 2015. Comparative genomic
761 analyses reveal a vast, novel network of nucleotide-centric systems in biological conflicts,
762 immunity and signaling. *Nucleic Acids Research,* 43**,** 10633-10654.
763 CHAKRABARTI, S., JAYACHANDRAN, U., BONNEAU, F., FIORINI, F., BASQUIN, C., DOMCKE, S., LE HIR, H. &
764 CONTI, E. 2011. Molecular mechanisms for the RNA-dependent ATPase activity of Upf1 and its
765 regulation by Upf2. *Mol Cell,* 41**,** 693-703.
766 CHANG, Y. W., SUN, Y. J., WANG, C. & HSIAO, C. D. 2008. Crystal structures of the 70-kDa heat shock
767 proteins in domain disjoining conformation. *J Biol Chem,* 283**,** 15502-11.
768 CHAVEZ, D. A., GREER, B. H. & EICHMAN, B. F. 2018. The HIRAN domain of helicase-like transcription
769 factor positions the DNA translocase motor to drive efficient DNA fork regression. *J Biol Chem,*
770 293**,** 8484-8494.
771 CHENG, Z., MUHLRAD, D., LIM, M. K., PARKER, R. & SONG, H. 2007. Structural and functional insights
772 into the human Upf1 helicase core. *Embo j,* 26**,** 253-64.
773 COLICELLI, J. 2004. Human RAS superfamily proteins and related GTPases. *Sci STKE,* 2004**,** Re13.
774 DAS, U. & SHUMAN, S. 2013. 2'-Phosphate cyclase activity of RtcA: a potential rationale for the operon
775 organization of RtcA with an RNA repair ligase RtcB in Escherichia coli and other bacterial taxa.
776 *Rna,* 19**,** 1355-62.

DILA, D., SUTHERLAND, E., MORAN, L., SLATKO, B. & RALEIGH, E. A. 1990. Genetic and sequence organization of the mcrBC locus of Escherichia coli K-12. *Journal of Bacteriology,* 172**,** 4888.

DOVAS, A. & COUCHMAN, J. R. 2005. RhoGDI: multiple functions in the regulation of Rho family GTPase activities. *Biochem J,* 390**,** 1-9.

EDGAR, R. C. 2004. MUSCLE: a multiple sequence alignment method with reduced time and space complexity. *BMC bioinformatics,* 5**,** 113-113.

ERZBERGER, J. P. & BERGER, J. M. 2006. Evolutionary relationships and structural mechanisms of AAA+ proteins. *Annu Rev Biophys Biomol Struct,* 35**,** 93-114.

FAIRMAN-WILLIAMS, M. E., GUENTHER, U. P. & JANKOWSKY, E. 2010. SF1 and SF2 helicases: family matters. *Curr Opin Struct Biol,* 20**,** 313-24.

FIRE, A., XU, S., MONTGOMERY, M. K., KOSTAS, S. A., DRIVER, S. E. & MELLO, C. C. 1998. Potent and specific genetic interference by double-stranded RNA in Caenorhabditis elegans. *Nature,* 391**,** 806-11.

FLEISCHMAN, R. A., CAMBELL, J. L. & RICHARDSON, C. C. 1976. Modification and restriction of T-even bacteriophages. In vitro degradation of deoxyribonucleic acid containing 5-hydroxymethylctosine. *J Biol Chem,* 251**,** 1561-70.

GABLER, F., NAM, S. Z., TILL, S., MIRDITA, M., STEINEGGER, M., SÖDING, J., LUPAS, A. N. & ALVA, V. 2020. Protein Sequence Analysis Using the MPI Bioinformatics Toolkit. *Curr Protoc Bioinformatics,* 72**,** e108.

GAO, L., ALTAE-TRAN, H., BOHNING, F., MAKAROVA, K. S., SEGEL, M., SCHMID-BURGK, J. L., KOOB, J., WOLF, Y. I., KOONIN, E. V. & ZHANG, F. 2020. Diverse enzymatic activities mediate antiviral immunity in prokaryotes. *Science,* 369**,** 1077-1084.

GASIUNAS, G., BARRANGOU, R., HORVATH, P. & SIKSNYS, V. 2012. Cas9-crRNA ribonucleoprotein complex mediates specific DNA cleavage for adaptive immunity in bacteria. *Proc Natl Acad Sci U S A,* 109**,** E2579-86.

GENSCHIK, P., DRABIKOWSKI, K. & FILIPOWICZ, W. 1998. Characterization of the Escherichia coli RNA 3'-terminal phosphate cyclase and its sigma54-regulated operon. *J Biol Chem,* 273**,** 25516-26.

GOEDERS, N., DRÈZE, P. L. & VAN MELDEREN, L. 2013. Relaxed cleavage specificity within the RelE toxin family. *J Bacteriol,* 195**,** 2541-9.

GOLDFARB, T., SBERRO, H., WEINSTOCK, E., COHEN, O., DORON, S., CHARPAK-AMIKAM, Y., AFIK, S., OFIR, G. & SOREK, R. 2015. BREX is a novel phage resistance system widespread in microbial genomes. *Embo j,* 34**,** 169-83.

GORBALENYA, A. E. & KOONIN, E. V. 1993. Helicases: amino acid sequence comparisons and structure-function relationships. *Current Opinion in Structural Biology,* 3**,** 419-429.

GUCINSKI, G. C., MICHALSKA, K., GARZA-SÁNCHEZ, F., ESCHENFELDT, W. H., STOLS, L., NGUYEN, J. Y., GOULDING, C. W., JOACHIMIAK, A. & HAYES, C. S. 2019. Convergent Evolution of the Barnase/EndoU/Colicin/RelE (BECR) Fold in Antibacterial tRNase Toxins. *Structure,* 27**,** 1660-1674.e5.

GUGLIELMINI, J. & VAN MELDEREN, L. 2011. Bacterial toxin-antitoxin systems: Translation inhibitors everywhere. *Mob Genet Elements,* 1**,** 283-290.

GUTMANN, S., HAEBEL, P. W., METZINGER, L., SUTTER, M., FELDEN, B. & BAN, N. 2003. Crystal structure of the transfer-RNA domain of transfer-messenger RNA in complex with SmpB. *Nature,* 424**,** 699-703.

GUYOMAR, C., D'URSO, G., CHAT, S., GIUDICE, E. & GILLET, R. 2021. Structures of tmRNA and SmpB as they transit through the ribosome. *Nat Commun,* 12**,** 4909.

HALABY, D. M., POUPON, A. & MORNON, J. 1999. The immunoglobulin fold family: sequence analysis and 3D structure comparisons. *Protein Eng,* 12**,** 563-71.

824 HAUSER, M., STEINEGGER, M. & SÖDING, J. 2016. MMseqs software suite for fast and deep clustering
825 and searching of large protein sequence sets. *Bioinformatics,* 32**,** 1323-1330.
826 HAZRA, D., CHAPAT, C. & GRAILLE, M. 2019. m^6A mRNA Destiny: Chained to the rhYTHm by the YTH-
827 Containing Proteins. *Genes,* 10**,** 49.
828 HEINEMANN, U. & ROSKE, Y. 2021. Cold-Shock Domains-Abundance, Structure, Properties, and Nucleic-
829 Acid Binding. *Cancers (Basel),* 13.
830 HIMENO, H., KURITA, D. & MUTO, A. 2014. tmRNA-mediated trans-translation as the major ribosome
831 rescue system in a bacterial cell. *Front Genet,* 5**,** 66.
832 HOLM, L. 2020. DALI and the persistence of protein shape. 29**,** 128-140.
833 HUGHES, K. J., CHEN, X., BURROUGHS, A. M., ARAVIND, L. & WOLIN, S. L. 2020. An RNA Repair Operon
834 Regulated by Damaged tRNAs. *Cell Rep,* 33**,** 108527.
835 IPSARO, J. J., HAASE, A. D., KNOTT, S. R., JOSHUA-TOR, L. & HANNON, G. J. 2012. The structural
836 biochemistry of Zucchini implicates it as a nuclease in piRNA biogenesis. *Nature,* 491**,** 279-283.
837 IRASTORTZA-OLAZIREGI, M. & AMSTER-CHODER, O. 2020. Coupled Transcription-Translation in
838 Prokaryotes: An Old Couple With New Surprises. *Front Microbiol,* 11**,** 624830.
839 ISHITA, J., MATVEY, K., LEONID, M., NATALIA, M., ANNA, S., ALEXANDR, K., SOFIA, M., KONSTANTIN, K.,
840 SERGEI, B., KIRA, S. M., EUGENE, V. K., KONSTANTIN, S. & EKATERINA, S. 2021. tRNA anticodon
841 cleavage by target-activated CRISPR-Cas13a effector. *bioRxiv***,** 2021.11.10.468108.
842 IYER, L. M., LEIPE, D. D., KOONIN, E. V. & ARAVIND, L. 2004. Evolutionary history and higher order
843 classification of AAA+ ATPases. *Journal of Structural Biology,* 146**,** 11-31.
844 JINEK, M., CHYLINSKI, K., FONFARA, I., HAUER, M., DOUDNA, J. A. & CHARPENTIER, E. 2012. A
845 Programmable Dual-RNA–Guided DNA Endonuclease in Adaptive Bacterial Immunity. *Science,*
846 337**,** 816-821.
847 JUMPER, J., EVANS, R., PRITZEL, A., GREEN, T., FIGURNOV, M., RONNEBERGER, O., TUNYASUVUNAKOOL,
848 K., BATES, R., ŽÍDEK, A., POTAPENKO, A., BRIDGLAND, A., MEYER, C., KOHL, S. A. A., BALLARD, A.
849 J., COWIE, A., ROMERA-PAREDES, B., NIKOLOV, S., JAIN, R., ADLER, J., BACK, T., PETERSEN, S.,
850 REIMAN, D., CLANCY, E., ZIELINSKI, M., STEINEGGER, M., PACHOLSKA, M., BERGHAMMER, T.,
851 BODENSTEIN, S., SILVER, D., VINYALS, O., SENIOR, A. W., KAVUKCUOGLU, K., KOHLI, P. &
852 HASSABIS, D. 2021. Highly accurate protein structure prediction with AlphaFold. *Nature,* 596**,**
853 583-589.
854 KALATHIYA, U., PADARIYA, M., PAWLICKA, K., VERMA, C. S., HOUSTON, D., HUPP, T. R. & ALFARO, J. A.
855 2019. Insights into the Effects of Cancer Associated Mutations at the UPF2 and ATP-Binding Sites
856 of NMD Master Regulator: UPF1. *Int J Mol Sci,* 20.
857 KAUFMANN, G. 2000. Anticodon nucleases. *Trends Biochem Sci,* 25**,** 70-4.
858 KAUR, G., BURROUGHS, A. M., IYER, L. M. & ARAVIND, L. 2020. Highly regulated, diversifying NTP-
859 dependent biological conflict systems with implications for the emergence of multicellularity.
860 *eLife,* 9**,** e52696.
861 KHADRIA, A. S. & SENES, A. 2013. The transmembrane domains of the bacterial cell division proteins
862 FtsB and FtsL form a stable high-order oligomer. *Biochemistry,* 52**,** 7542-50.
863 KISHOR, A., TANDUKAR, B., LY, Y. V., TOTH, E. A., SUAREZ, Y., BREWER, G. & WILSON, G. M. 2013. Hsp70
864 is a novel posttranscriptional regulator of gene expression that binds and stabilizes selected
865 mRNAs containing AU-rich elements. *Mol Cell Biol,* 33**,** 71-84.
866 KISHOR, A., WHITE, E. J. F., MATSANGOS, A. E., YAN, Z., TANDUKAR, B. & WILSON, G. M. 2017. Hsp70's
867 RNA-binding and mRNA-stabilizing activities are independent of its protein chaperone functions.
868 *J Biol Chem,* 292**,** 14122-14133.
869 KOONIN, E. V. & ARAVIND, L. 2002. Origin and evolution of eukaryotic apoptosis: the bacterial
870 connection. *Cell Death & Differentiation,* 9**,** 394-404.

871 KOONIN, E. V. & KRUPOVIC, M. 2019. Origin of programmed cell death from antiviral defense?
872 *Proceedings of the National Academy of Sciences,* 116**,** 16167.
873 KOONIN, E. V. & ZHANG, F. 2017. Coupling immunity and programmed cell suicide in prokaryotes: Life-
874 or-death choices. *BioEssays,* 39**,** e201600186.
875 KOTTA-LOIZOU, I., GIULIANO, M. G., JOVANOVIC, M., SCHAEFER, J., YE, F., ZHANG, N., IRAKLEIDI, D. A.,
876 LIU, X., ZHANG, X., BUCK, M. & ENGL, C. 2022. The RNA repair proteins RtcAB regulate
877 transcription activator RtcR via its CRISPR-associated Rossmann fold domain. *iScience,* 25**,**
878 105425.
879 LAGANECKAS, M., MARGELEVICIUS, M. & VENCLOVAS, C. 2011. Identification of new homologs of PD-
880 (D/E)XK nucleases by support vector machines trained on data derived from profile-profile
881 alignments. *Nucleic Acids Res,* 39**,** 1187-96.
882 LIAO, S., SUN, H. & XU, C. 2018. YTH Domain: A Family of N6-methyladenosine (m6A) Readers.
883 *Genomics, Proteomics & Bioinformatics,* 16**,** 99-107.
884 LOENEN, W. A., DRYDEN, D. T., RALEIGH, E. A., WILSON, G. G. & MURRAY, N. E. 2014. Highlights of the
885 DNA cutters: a short history of the restriction enzymes. *Nucleic Acids Res,* 42**,** 3-19.
886 LURIA, S. E. & HUMAN, M. L. 1952. A nonhereditary, host-induced variation of bacterial viruses. *J*
887 *Bacteriol,* 64**,** 557-69.
888 MACDONALD, E., STRAHL, H., BLOWER, T. R., PALMER, T. & MARIANO, G. 2022. Shield co-opts an RmuC
889 domain to mediate phage defence across Pseudomonas species. 2022.11.04.515146.
890 MAKAROVA, K. S., ANANTHARAMAN, V., ARAVIND, L. & KOONIN, E. V. 2012. Live virus-free or die:
891 coupling of antivirus immunity and programmed suicide or dormancy in prokaryotes. *Biology*
892 *direct,* 7**,** 40-40.
893 MAKAROVA, K. S., GRISHIN, N. V., SHABALINA, S. A., WOLF, Y. I. & KOONIN, E. V. 2006. A putative RNA-
894 interference-based immune system in prokaryotes: computational analysis of the predicted
895 enzymatic machinery, functional analogies with eukaryotic RNAi, and hypothetical mechanisms
896 of action. *Biology Direct,* 1**,** 7.
897 MAKAROVA, K. S., TIMINSKAS, A., WOLF, Y. I., GUSSOW, A. B., SIKSNYS, V., VENCLOVAS, Č. & KOONIN, E.
898 V. 2020a. Evolutionary and functional classification of the CARF domain superfamily, key sensors
899 in prokaryotic antivirus defense. *Nucleic Acids Res,* 48**,** 8828-8847.
900 MAKAROVA, K. S., WOLF, Y. I., IRANZO, J., SHMAKOV, S. A., ALKHNBASHI, O. S., BROUNS, S. J. J.,
901 CHARPENTIER, E., CHENG, D., HAFT, D. H., HORVATH, P., MOINEAU, S., MOJICA, F. J. M., SCOTT,
902 D., SHAH, S. A., SIKSNYS, V., TERNS, M. P., VENCLOVAS, Č., WHITE, M. F., YAKUNIN, A. F., YAN,
903 W., ZHANG, F., GARRETT, R. A., BACKOFEN, R., VAN DER OOST, J., BARRANGOU, R. & KOONIN, E.
904 V. 2020b. Evolutionary classification of CRISPR–Cas systems: a burst of class 2 and derived
905 variants. *Nature Reviews Microbiology,* 18**,** 67-83.
906 MARIANI, V., BIASINI, M., BARBATO, A. & SCHWEDE, T. 2013. lDDT: a local superposition-free score for
907 comparing protein structures and models using distance difference tests. *Bioinformatics,* 29**,**
908 2722-2728.
909 MAYER, M. P. 2021. The Hsp70-Chaperone Machines in Bacteria. *Front Mol Biosci,* 8**,** 694012.
910 MCMAHON, S. A., ZHU, W., GRAHAM, S., RAMBO, R., WHITE, M. F. & GLOSTER, T. M. 2020. Structure
911 and mechanism of a Type III CRISPR defence DNA nuclease activated by cyclic oligoadenylate.
912 *Nature Communications,* 11**,** 500.
913 MENDEZ, A. S., VOGT, C., BOHNE, J. & GLAUNSINGER, B. A. 2018. Site specific target binding controls
914 RNA cleavage efficiency by the Kaposi's sarcoma-associated herpesvirus endonuclease SOX.
915 *Nucleic Acids Research,* 46**,** 11968-11979.
916 MILLMAN, A., MELAMED, S., AMITAI, G. & SOREK, R. 2020. Diversity and classification of cyclic-
917 oligonucleotide-based anti-phage signalling systems. *Nature Microbiology,* 5**,** 1608-1615.

918 MORSE, J. C., GIRODAT, D., BURNETT, B. J., HOLM, M., ALTMAN, R. B., SANBONMATSU, K. Y., WIEDEN,
919 H.-J. & BLANCHARD, S. C. 2020. Elongation factor-Tu can repetitively engage aminoacyl-tRNA
920 within the ribosome during the proofreading stage of tRNA selection. *Proceedings of the*
921 *National Academy of Sciences,* 117**,** 3610-3620.
922 NATARAJAN, K., MAGE, M. G. & MARGULIES, D. H. 2015. Immunoglobulin Superfamily. *Encyclopedia of*
923 *Life Sciences.*
924 NEUWALD, A. F., ARAVIND, L., SPOUGE, J. L. & KOONIN, E. V. 1999. AAA+: A class of chaperone-like
925 ATPases associated with the assembly, operation, and disassembly of protein complexes.
926 *Genome Res,* 9**,** 27-43.
927 NIRWAN, N., ITOH, Y., SINGH, P., BANDYOPADHYAY, S., VINOTHKUMAR, K. R., AMUNTS, A. &
928 SAIKRISHNAN, K. 2019. Structure-based mechanism for activation of the AAA+ GTPase McrB by
929 the endonuclease McrC. *Nature Communications,* 10**,** 3058.
930 NIU, Y., SUZUKI, H., HOSFORD, C. J., WALZ, T. & CHAPPIE, J. S. 2020. Structural asymmetry governs the
931 assembly and GTPase activity of McrBC restriction complexes. *Nat Commun,* 11**,** 5907.
932 OFIR, G., MELAMED, S., SBERRO, H., MUKAMEL, Z., SILVERMAN, S., YAAKOV, G., DORON, S. & SOREK, R.
933 2018. DISARM is a widespread bacterial defence system with broad anti-phage activities. *Nature*
934 *Microbiology,* 3**,** 90-98.
935 PANNE, D., RALEIGH, E. A. & BICKLE, T. A. 1999. The McrBC endonuclease translocates DNA in a reaction
936 dependent on GTP hydrolysis. *J Mol Biol,* 290**,** 49-60.
937 PARK, H. H., LO, Y. C., LIN, S. C., WANG, L., YANG, J. K. & WU, H. 2007. The death domain superfamily in
938 intracellular signaling of apoptosis and inflammation. *Annu Rev Immunol,* 25**,** 561-86.
939 PATIL, D. P., PICKERING, B. F. & JAFFREY, S. R. 2018. Reading m6A in the Transcriptome: m6A-Binding
940 Proteins. *Trends in Cell Biology,* 28**,** 113-127.
941 PEDERSEN, K., ZAVIALOV, A. V., PAVLOV, M. Y., ELF, J., GERDES, K. & EHRENBERG, M. 2003. The bacterial
942 toxin RelE displays codon-specific cleavage of mRNAs in the ribosomal A site. *Cell,* 112**,** 131-40.
943 PETTERSEN, E. F., GODDARD, T. D., HUANG, C. C., MENG, E. C., COUCH, G. S., CROLL, T. I., MORRIS, J. H.
944 & FERRIN, T. E. 2021. UCSF ChimeraX: Structure visualization for researchers, educators, and
945 developers. 30**,** 70-82.
946 PIEPER, U., SCHWEITZER, T., GROLL, D. H., GAST, F. U. & PINGOUD, A. 1999. The GTP-binding domain of
947 McrB: more than just a variation on a common theme? *J Mol Biol,* 292**,** 547-56.
948 PILLON, M. C., GORDON, J., FRAZIER, M. N. & STANLEY, R. E. 2021. HEPN RNases - an emerging class of
949 functionally distinct RNA processing and degradation enzymes. *Crit Rev Biochem Mol Biol,* 56**,**
950 88-108.
951 PRICE, M. N., DEHAL, P. S. & ARKIN, A. P. 2010. FastTree 2 – Approximately Maximum-Likelihood Trees
952 for Large Alignments. *PLOS ONE,* 5**,** e9490.
953 RALEIGH, E. A. 1992. Organization and function of the mcrBC genes of Escherichia coli K-12. *Mol*
954 *Microbiol,* 6**,** 1079-86.
955 RALEIGH, E. A., TRIMARCHI, R. & REVEL, H. 1989. Genetic and physical mapping of the mcrA (rglA) and
956 mcrB (rglB) loci of Escherichia coli K-12. *Genetics,* 122**,** 279-296.
957 ROBERT, C. E. 2022. High-accuracy alignment ensembles enable unbiased assessments of sequence
958 homology and phylogeny. *bioRxiv***,** 2021.06.20.449169.
959 SHIGEMATSU, M., KAWAMURA, T. & KIRINO, Y. 2018. Generation of 2',3'-Cyclic Phosphate-Containing
960 RNAs as a Hidden Layer of the Transcriptome. *Front Genet,* 9**,** 562.
961 SÖDING, J. 2004. Protein homology detection by HMM–HMM comparison. *Bioinformatics,* 21**,** 951-960.
962 SÖDING, J., REMMERT, M., BIEGERT, A. & LUPAS, A. N. 2006. HHsenser: exhaustive transitive profile
963 search using HMM–HMM comparison. *Nucleic Acids Research,* 34**,** W374-W378.

964 SONGAILIENE, I., JUOZAPAITIS, J., TAMULAITIENE, G., RUKSENAITE, A., ŠULČIUS, S., SASNAUSKAS, G.,
965 VENCLOVAS, Č. & SIKSNYS, V. 2020. HEPN-MNT Toxin-Antitoxin System: The HEPN Ribonuclease
966 Is Neutralized by OligoAMPylation. *Molecular Cell,* 80**,** 955-970.e7.
967 STOCK, A. M., ROBINSON, V. L. & GOUDREAU, P. N. 2000. Two-component signal transduction. *Annu Rev*
968 *Biochem,* 69**,** 183-215.
969 SUKACKAITE, R., GRAZULIS, S., TAMULAITIS, G. & SIKSNYS, V. 2012. The recognition domain of the
970 methyl-specific endonuclease McrBC flips out 5-methylcytosine. *Nucleic acids research,* 40**,**
971 7552-7562.
972 SUTHERLAND, E., COE, L. & RALEIGH, E. A. 1992. McrBC: a multisubunit GTP-dependent restriction
973 endonuclease. *J Mol Biol,* 225**,** 327-48.
974 SWARTS, D. C., MAKAROVA, K., WANG, Y., NAKANISHI, K., KETTING, R. F., KOONIN, E. V., PATEL, D. J. &
975 VAN DER OOST, J. 2014. The evolutionary journey of Argonaute proteins. *Nature structural &*
976 *molecular biology,* 21**,** 743-753.
977 TANAKA, N. & SHUMAN, S. 2011. RtcB is the RNA ligase component of an Escherichia coli RNA repair
978 operon. *J Biol Chem,* 286**,** 7727-7731.
979 TSUTAKAWA, S. E., JINGAMI, H. & MORIKAWA, K. 1999. Recognition of a TG Mismatch: The Crystal
980 Structure of Very Short Patch Repair Endonuclease in Complex with a DNA Duplex. *Cell,* 99**,** 615-
981 623.
982 VAN DEN BERG, D. F., VAN DER STEEN, B. A., COSTA, A. R. & BROUNS, S. J. J. 2023. Phage tRNAs evade
983 tRNA-targeting host defenses through anticodon loop mutations. *eLife,* 12**,** e85183.
984 VAN KEMPEN, M., KIM, S. S., TUMESCHEIT, C., MIRDITA, M., LEE, J., GILCHRIST, C. L. M., SÖDING, J. &
985 STEINEGGER, M. 2023. Fast and accurate protein structure search with Foldseek. *Nature*
986 *Biotechnology*.
987 WEIGELE, P. & RALEIGH, E. 2016. Biosynthesis and Function of Modified Bases in Bacteria and Their
988 Viruses. *Chemical reviews,* 116.
989 WILLMUND, F., DEL ALAMO, M., PECHMANN, S., CHEN, T., ALBANÈSE, V., DAMMER, E. B., PENG, J. &
990 FRYDMAN, J. 2013. The cotranslational function of ribosome-associated Hsp70 in eukaryotic
991 protein homeostasis. *Cell,* 152**,** 196-209.
992 YAMAMOTO, S., SUBEDI, G. P., HANASHIMA, S., SATOH, T., OTAKA, M., WAKUI, H., SAWADA, K.-I.,
993 YOKOTA, S.-I., YAMAGUCHI, Y., KUBOTA, H. & ITOH, H. 2014. ATPase Activity and ATP-
994 dependent Conformational Change in the Co-chaperone HSP70/HSP90-organizing Protein
995 (HOP)*. *Journal of Biological Chemistry,* 289**,** 9880-9886.
996 ZHOU, C., POURMAL, S. & PAVLETICH, N. P. 2015. Dna2 nuclease-helicase structure, mechanism and
997 regulation by Rpa. *eLife,* 4**,** e09832.
998 ZHU, W., MCQUARRIE, S., GRÜSCHOW, S., MCMAHON, S. A., GRAHAM, S., GLOSTER, T. M. & WHITE, M.
999 F. 2021. The CRISPR ancillary effector Can2 is a dual-specificity nuclease potentiating type III
1000 CRISPR defence. *Nucleic Acids Research,* 49**,** 2777-2789.
1001 ZIMMER, C., VON GABAIN, A. & HENICS, T. 2001. Analysis of sequence-specific binding of RNA to Hsp70
1002 and its various homologs indicates the involvement of N- and C-terminal interactions. *Rna,* 7**,**
1003 1628-37.
1004 ZIMMERMANN, L., STEPHENS, A., NAM, S.-Z., RAU, D., KÜBLER, J., LOZAJIC, M., GABLER, F., SÖDING, J.,
1005 LUPAS, A. N. & ALVA, V. 2018. A Completely Reimplemented MPI Bioinformatics Toolkit with a
1006 New HHpred Server at its Core. *Journal of Molecular Biology,* 430**,** 2237-2243.

1007